From *cereus* to anthrax and back again: The role of the PlcR regulator in the "cross-over" strain *Bacillus cereus* G9241

Shathviga Manoharan[1], Grace Taylor-Joyce[1], Thomas A. Brooker[1], Carmen Sara Hernandez-Rodriguez[2], Alexia Hapeshi[1], Victoria Baldwin[3], Les Baillie[4], Petra C. F. Oyston[3] and Nicholas R. Waterfield[1]♦.

[1]Division of Biomedical Sciences, Warwick Medical School, University of Warwick, Gibbet Hill Road, Coventry, CV4 7AL, United Kingdom

[2]Dpto. Microbiología y Ecología, Instituto BIOTECMED, Universitat de València, 46100 Burjassot, Spain.

[3]CBR Division, Dstl Porton Down, Salisbury, SP4 0JQ, United Kingdom

[4]School of Pharmacy and Pharmaceutical Sciences, Cardiff University, CF10 3AT, Cardiff, United Kingdom

♦ corresponding author (n.r.waterfield@warwick.ac.uk)

ABSTRACT

Bacillus cereus G9241 was isolated from a Louisiana welder suffering from an anthrax-like infection. The organism carries two transcriptional regulators that have previously been proposed to be incompatible with each other: the pleiotropic transcriptional regulator PlcR found in most members of the *Bacillus cereus* group but truncated in all *Bacillus anthracis* isolates, and the anthrax toxin regulator AtxA found in all *B. anthracis* strains and a few *B. cereus* sensu stricto strains. Here we report cytotoxic and haemolytic activity of cell free *B. cereus* G9241 culture supernatants cultured at 25 °C to various eukaryotic cells. However, this is not observed at the mammalian infection relevant temperature 37 °C, behaving much like the supernatants generated by *B. anthracis*. Using a combination of genetic and proteomic approaches to understand this unique phenotype, we identified several PlcR-regulated toxins to be secreted highly at 25 °C compared to 37 °C. Furthermore, we demonstrate that differential expression of the protease involved in processing the PlcR quorum sensing activator molecule PapR appears to be the limiting step for the production of PlcR-regulated toxins at 37 °C, giving rise to the temperature-dependent haemolytic and cytotoxic activity of the culture supernatants. This study provides an insight on how *B. cereus* G9241 is able to 'switch' between *B. cereus* and *B. anthracis*–like phenotypes in a temperature-dependent manner, potentially accommodating the activities of both PlcR and AtxA.

KEYWORDS: *Bacillus cereus* G9241, PlcR regulon, virulence factors, secretome, haemolysin

37 # INTRODUCTION

38 The *Bacillus cereus* sensu lato complex is a group of genetically similar but phenotypically diverse
39 Gram-positive, soil-borne, rod-shaped bacteria (1,2), which includes the well-studied *Bacillus anthracis*
40 *and Bacillus cereus*. *B. anthracis* is the etiological agent of anthrax (3) while *B. cereus* can colonise
41 hosts as diverse as insects (4) and humans, in which many strains can cause serious foodborne illness
42 (5). Most members of the *B. cereus* group express the chromosomally encoded transcriptional regulator
43 PlcR (Phospholipase C regulator), which controls the expression of many secreted degradative
44 enzymes and toxins (6). However, the *plcR* gene in all *B. anthracis* isolates contains a point mutation,
45 which frameshifts the gene and thus renders it non-functional (7). It has been proposed that the
46 acquisition of AtxA, the mammalian responsive transcriptional regulator involved in expressing anthrax
47 toxins, is incompatible with the activity of PlcR, leading to a selection for PlcR mutation and inactivation
48 (7,8). Interestingly, a *B. cereus-B. anthracis* "cross-over" strain designated *B. cereus* G9241
49 (hereon referred to as *Bc*G9241) encodes intact copies of both *atxA* and *plcR* genes (9), suggesting
50 this incompatibility dogma is not as straightforward as first suggested.
51
52 *Bc*G9241 was isolated from a Louisiana welder, who was hospitalised with a respiratory infection
53 resulting in a case of potentially lethal pneumonia (9). Symptoms were similar to those of inhalational
54 anthrax. The patient also suffered with haemoptysis. *Bc*G9241 possesses three extrachromosomal
55 elements: pBCX01, pBC210 and pBFH_1 (9,10). The plasmid pBCX01 shares 99.6% sequence
56 homology with the plasmid pXO1 from *B. anthracis* strains. pBCX01 encodes the protective antigen
57 (PA), lethal factor (LF), oedema factor (EF) and the AtxA1 regulator. The second plasmid pBC210
58 (previously known as pBC218) encodes for the *B. cereus* exo-polysaccharide (BPS) capsule
59 biosynthesis genes, *bpsXABCDEFGH* (9). A novel toxin named certhrax is also encoded on the
60 pBC210 plasmid (11,12), which has 31% amino acid sequence similarity with the LF from *B. anthracis*.
61 Moreover, pBC210 encodes gene products with amino acid sequences bearing homology to AtxA and
62 PA of *B. anthracis* (9). Subsequently these genes have been named *atxA2* and *pagA2*. The third
63 extrachromosomal element pBFH_1 (previously known as pBClin29) is a linear phagemid (9). Although
64 the sequence is available for pBFH_1, it is not known if it contributes to the lifestyle of *Bc*G9241. Our
65 group demonstrated by transmission electron microscopy that the pBFH_1 phage could be produced
66 and released into the supernatant (13). The shape of the phage particles and the dimensions of the tail
67 and head appeared to be consistent with the Siphoviridae family (14), suggesting the pBFH_1 is a
68 Siphoviridae phage. Phenotypically, *Bc*G9241 is haemolytic and resistant to γ-phage like other *B.*
69 *cereus* strains (9). Further phenotypic and genetic analyses suggested that *Bc*G9241 should be
70 considered a member of the *B. cereus* sensu stricto group as it does not encode a point mutation in the
71 *plcR* gene indicative of a *B. anthracis* strain (8).
72
73 PlcR controls the expression of many secreted enzymes and toxins (6,7,15), with at least 45 regulated
74 genes found in *B. cereus* type strain ATCC 14579 (16), hereon referred to as *Bc*ATCC14579. These
75 secreted proteins, which contribute significantly to virulence in mice and insects (17,18), include
76 haemolysins, enterotoxins, proteases, collagenases and phospholipases (15). Activation of PlcR

77 requires the binding of a secreted, processed and reimported form of the signalling peptide PapR (6,19–
78 21). The *papR* gene is located downstream of *plcR* and encodes a 48-amino acid protein. $PapR_{48}$ is
79 secreted from the cell via the Sec machinery and processed to a heptapeptide by the extracellular zinc
80 metalloprotease, NprB and potentially other extracellular proteases (22). The *nprB* gene is often tightly
81 linked to the *plcR-papR* operon, but in the opposite orientation (6,21,22). The processed form $PapR_7$ is
82 reimported into the bacterium by the oligopeptide permease (Opp) system (23). The processed form of
83 PapR can then bind and activate PlcR. The active PlcR-PapR complex binds to the palindromic operator
84 sequence (PlcR box: TATGNAN4TNCATA) found in the promoter regions of the regulon genes,
85 subsequently activating transcription of these genes (24–26). PlcR also positively auto-regulates its
86 own transcription, which can be repressed by the sporulation factor Spo0A, facilitated by two Spo0A
87 boxes flanking the PlcR box (27). Four distinct classes of PlcR-PapR systems have evolved and differ
88 by the 5 C-terminal amino acids of PapR, which bind to PlcR, with PapR from one group unable to
89 activate the transcriptional activity of PlcR from another (28).
90
91 The chromosome of *Bc*G9241 encodes a large range of intact exotoxin genes confirming the strain is
92 part of the sensu stricto group (9). Several of the toxin genes are likely to be regulated by PlcR, by
93 virtue of the presence of the PlcR-box sequence in the promoter regions (6). These include haemolysin
94 BL (Hbl) encoded by *hblCDAB*, the tripartite non-haemolytic enterotoxin (Nhe), encoded by *nheABC,*
95 and the enterotoxin cytotoxin K (CytK), encoded by *cytK*. These three toxins are all classed as
96 enterotoxins and have been isolated from patients suffering from food-borne, diarrhoeal infections (29–
97 31). Since isolating *Bc*G9241, cases of anthrax-like disease caused by other non-*B. anthracis* bacteria
98 have been reported, affecting both animals such as chimpanzees and gorillas in the Ivory Coast and
99 Cameroon during the early 2000s (32–36), in addition to humans (9,10,37–44). Some of these isolates
100 carry functional copies of *plcR* and *atxA* (recently reviewed in (45)); this warrants further investigation
101 into the role of PlcR in these strains, as the loss of PlcR activity has been proposed to be crucial in
102 anthrax disease caused by *B. anthracis*. So far, only one study on *Bc*G9241 has been carried out to
103 identify how PlcR, AtxA and their respective regulons are expressed. A microarray assay carried out by
104 (46) demonstrated that in *Bc*G9241 the *plcR* gene was ~2.4 fold more highly expressed in an aerobic
105 environment compared to when exposed to CO_2/bicarbonate, while in contrast, the *atxA1* gene showed
106 higher expression in CO_2 by ~5.6 fold. Understanding how the PlcR-PapR regulatory circuit acts in *B.*
107 *cereus-B. anthracis* "cross-over" strains may provide an insight into their evolution and give a more
108 complete picture of the phylogeny.
109
110 Here, we describe the temperature-dependent haemolytic and cytolytic activity of *Bc*G9241, caused by
111 PlcR-controlled toxins and proteases. We also identify the limiting step in the PlcR-PapR circuit involved
112 in preventing the expression of PlcR-regulated toxins at 37 °C. NprB is not involved in processing PapR
113 in *Bc*G9241 and other *B. cereus* strains carrying functional copies of both *plcR* and *atxA*. We
114 hypothesise that a change in the PlcR-PapR regulatory network in *Bc*G9241 may have allowed the
115 carriage of intact copies of both *plcR* and *atxA,* by virtue of a temperature-dependent suppression of
116 the PlcR-PapR circuit and the loss of the *nprB* gene.

117

118 # RESULTS

119

120 ***Bc*G9241 culture supernatants demonstrate temperature-dependent toxicity**
121 **against a range of eukaryotic cells.** It has been previously shown in other members of the *B.*
122 *cereus* group that PlcR regulates the secretion of multiple virulence proteins, such as cytolytic toxins
123 and enzymes involved in macromolecule degradation (16,47,48). We therefore tested the haemolytic
124 activity of cell free culture supernatants from *Bc*G9241 cultures grown at 25 ºC and 37 ºC to sheep
125 erythrocytes. We tested the effect of growth at 25 ºC and 37 ºC to partially emulate environmental and
126 mammalian host conditions, respectively. Filtered supernatants were extracted from cultures grown to
127 exponential phase (OD_{600}=0.5) and stationary phase (OD_{600}=1.5). From 25 °C cultures, the
128 supernatants from exponential and stationary phases demonstrated haemolytic activity to red blood
129 cells (RBCs), above the 75% level by comparison to the expected lysis from the positive control (1%
130 Triton X100) (**Fig 1**). In contrast, supernatants from *Bc*G9241 grown at 37 ºC showed very little lytic
131 activity (**Fig 1**). This led us to the hypothesis that *Bc*G9241 'switches' its phenotype from a haemolytic
132 *B. cereus*-like phenotype at 25 °C to a non-haemolytic *B. anthracis*-like phenotype at 37 °C.

133

134 We expanded the study to test the toxicity of cell free culture supernatants from a range of *Bacillus*
135 cultures grown at 25 ºC against *ex vivo Manduca sexta* haemocytes. Filtered supernatants were
136 extracted from cultures grown for 16 h. Microscopic examination showed that supernatants from the
137 reference strain *Bc*ATCC14579, *Bc*G9241 and *Bc*G9241 ΔpBCX01 (in which the plasmid had been
138 cured) caused extensive lysis of the *M. sexta* haemocytes (**Fig S1A**). In contrast, supernatants from
139 *Bacillus thuringiensis* 407 Cry^- *ΔplcR* (*Bt ΔplcR*) mutant strain were innocuous, showing no difference
140 from the negative buffer control (**Fig S1A**). *Bt ΔplcR* is an accepted Δ*plcR B. cereus* model as the
141 crystal toxin plasmid has been cured (27). The cytotoxicity observed with *Bc*G9241 and *Bc*G9241
142 ΔpBCX01 indicated that cytotoxins were secreted by both strains and is possibly unaffected by the
143 presence of pBCX01 plasmid at 25 ºC (**Fig S1A**).

144

145 We quantified the effect of supernatants from these same strains using haemocyte cell viability assays.
146 We also expanded the study to include supernatants from the *B. anthracis* Sterne strain, which lacks
147 the pXO2 plasmid (hereon referred to as *Ba* St). Like all *B. anthracis* strains, *Ba* St has a frame-shifted
148 copy of the *plcR* gene. From 25 ºC grown cultures, we observed cytotoxicity responses consistent with
149 the microscopic examinations (**Fig S1B**), with the supernatants of *Bc*ATCC14579, *Bc*G9241 and
150 *Bc*G9241 ΔpBCX01, all showing potent toxicity. In contrast, supernatants from *Ba* St and *Bt ΔplcR*
151 showed little or no cytotoxicity (**Fig S1B**). However, when grown at 37 ºC, cytotoxicity of *Bc*G9241 and
152 BcG9241 ΔpBCX01 supernatants was highly attenuated, to levels no different from those of the *Ba* St
153 and *Bt ΔplcR* supernatants (**Fig S1C**). Cytotoxicity of the *Bc*ATCC14579 supernatant was still observed
154 at 37 ºC (**Fig S1C**). Temperature-dependent cytotoxic activity of *Bc*G9241 and *Bc*G9241 ΔpBCX01
155 supernatants were also observed in a range of mammalian cells including T2-lymphocytes,

156 polymorphonuclear leukocytes and macrophages (using supernatant extracted from *Bacillus* cultures
157 grown for 16 h), which re-capitulated the trend seen with the insect haemocytes (**Fig S2**).

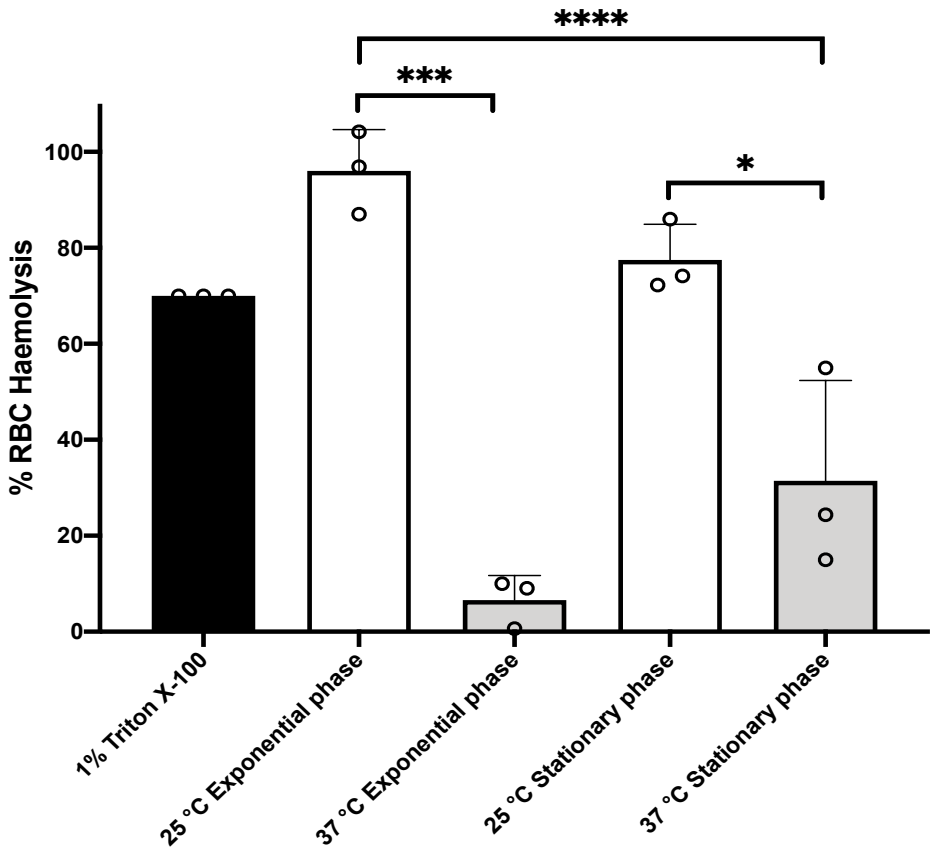

158 **Figure 1: *Bc*G9241 supernatant is significantly more toxic to sheep RBCs, when extracted from**
159 **a 25 °C grown culture compared to a 37 °C grown culture.** The haemolysis assay was conducted
160 by incubating *Bc*G9241 supernatant with 4% RBCs for 1 hour at 37 °C. The OD_{540} was measured, and
161 RBC lysis was calculated as a % of expected RBC lysis by Triton X-100 (1% v/v). Stars above columns
162 represent significance levels. * denotes an unpaired t test with a p-value of 0.0232; *** denotes a
163 Welch's t test with a p-value of 0.0003; **** denotes an ordinary one-way ANOVA with a p-value of
164 <0.0001. Error bars denote one standard deviation, and all samples were to an n=3.
165
166
167 **Temperature and growth phase-dependent proteomic analysis of *Bc*G9241**
168 **culture supernatants.** In order to investigate the potential cytolytic and haemolytic factors
169 secreted by *Bc*G9241, we analysed the proteomic profiles of supernatants from cultures grown at 25
170 °C and 37 °C in LB broth, taken from both mid-exponential (OD_{600} = 0.5) and stationary growth phases.
171 For stationary phase, *Bc*G9241 cultures supernatant were extracted after 10 hours growth at 25 °C and
172 after 7 hours growth at 37°C (13). Proteins were run through nanoLC-ESI-MS and peptide reads were
173 counted using MaxQuant (Max Planck Institute). Comparisons were made using the Perseus software

174 (Max Planck Institute) and plotted as the difference in proteins expressed between the two
175 temperatures. The full datasets generated can be seen in the **Supplementary Dataset S1 and S2.**
176
177 A principal component analysis (PCA) was generated to show the variance between all biological
178 replicates of the *Bc*G9241 supernatants collected from both exponential- and stationary phases. The
179 PCA plots revealed that protein extracts from the exponential phase supernatants overlap with each
180 other, not forming distinct clusters and are highly reproducible (**Fig S3**). The plot also showed that
181 growth temperature affected the protein profiles more significantly at stationary phase compared to
182 exponential phase (**Fig S3**). Furthermore, protein profiles extracted from stationary phase growth at 37
183 °C were more variable than those from other conditions (**Fig S3**).
184
185 **A diverse and abundant toxin "profile" was secreted at 25 °C, while high levels of phage proteins**
186 **were secreted at 37 °C during exponential growth phase of *Bc*G9241.** With the cut-off criteria of p-
187 value < 0.05 and a minimum 2-fold change in protein level, 33 supernatant proteins were identified as
188 being significantly more abundant at 25 °C compared to 37 °C. Of these, 11 of the 12 most highly
189 expressed are known toxin homologs (**Table 1** and **Fig S4**). This included all components of the Hbl
190 toxin encoded by the *hbl* operon AQ16_4930 – 4933 **(Fig S4-purple arrows)**. Other known cytotoxic
191 proteins were also abundant in the supernatant at 25 °C compared to 37 °C, including the Nhe toxin
192 encoded by the *nhe* operon AQ16_658 – 660 (**Fig S4-green arrows**), a collagenase (AQ16_1941), a
193 thermolysin metallopeptidase (AQ16_5317), phospholipase C (Plc, AQ16_1823) and CytK
194 (AQ16_1392).
195
196 Conversely, at 37 °C, the secretome contained negligible levels of these cytotoxic proteins (if present
197 at all). There was, however, an abundance of phage capsid proteins encoded by the pBFH_1 phagemid
198 at 37 °C compared to 25 °C (**Fig S4-black arrows**). More specifically 25 proteins were found to be
199 more abundant in the secretome at 37 °C compared to 25 °C. The 10 most abundant proteins at 37 °C
200 compared to 25 °C were encoded by the pBFH_1 phagemid (**Table 1**). Proteins from an operon of
201 WxL-domain cell wall-binding proteins were also seen to be more abundant at 37 °C compared to 25
202 °C (AQ16_3217 – 3219).
203
204 **The temperature dependent *Bc*G9241 secretome at stationary growth phase.** Between 25 °C and
205 37 °C, 51 proteins showed temperature dependent differences (**Fig 2B**). Unlike the mid-exponential
206 observations, the more abundant proteins in the 25 °C stationary phase supernatants were not all
207 cytotoxins, although several enzymes were present (**Table 1**). In fact, of the 11 toxins seen to be more
208 abundant at 25 °C during exponential phase growth, only AQ16_5317 was identified at higher levels at
209 25 °C during stationary phase. This is a thermolysin metallopeptidase, which has a PlcR-box present
210 in the promoter region (**Table S1**), and is over 200-fold more abundant at 25 °C. The relevance of this
211 is discussed below. Several of the more abundant proteins (e.g. AQ16_3254, 4226, 374) identified were
212 likely cellular proteins, possibly indicating greater autolysis at 25 °C compared to 37 °C. The top 5
213 proteins more abundant in 37 °C compared to 25 °C supernatants were all extracellular enzymes

214 including two chitinases, a hydrolase, a glucanase and a collagenase (**Table 1**). In addition, a matrixin
215 family protein (AQ16_4915), another extracellular enzyme, was also identified as 4.3 log2-fold higher
216 at 37 °C. Again, we saw cellular components including 50S ribosome subunit proteins and RecA, which
217 possibly signified cell lysis. Only one of the phage capsid proteins identified as higher at 37 °C in the
218 exponential phase secretome, Gp34 (AQ16_5824), was significantly higher at 37 °C in stationary
219 phase.
220
221
222 **Table 1:** The 15 most abundant toxins at higher levels at the two temperature in the secretome of
223 *Bc*G9241 during exponential growth and stationary phase. The significance cut-off criteria used was a
224 p-value of <0.05 and a minimum of a 2-fold change in protein level.
225

Log_2-Fold Change	25 °C > 37 °C at exponential phase	Gene	Gene Loci (AQ16_)
6.46	Haemolysin BL lytic component L2		4931
5.88	Non-haemolytic enterotoxin binding component	*nheC*	658
5.67	Hemolysin BL-binding component	*hblA*	4932
4.41	Collagenase family protein		1941
4.31	Extracellular ribonuclease	*bsn*	4754
3.98	Hemolysin BL-binding component	*hblB*	4933
3.93	Non-hemolytic enterotoxin lytic component L2	*nheA*	660
3.84	Thermolysin metallopeptidase, catalytic domain protein		5317
3.77	Non-hemolytic enterotoxin lytic component L1	*nheB*	659
3.57	Haemolysin BL lytic component L1		4930
3.20	Phospholipase C	*olc*	1823
2.69	Cytotoxin K	*cytK*	1392
2.49	THUMP domain protein		931
2.44	Probable butyrate kinase	*buk*	3880
2.42	DEAD-box ATP-dependent RNA helicase	*cshA*	2258
	37 °C > 25 °C at exponential phase		
5.27	Phage family protein	*gp49*	5822
4.96	Putative phage major capsid protein	*gp34*	5824
4.53	Prophage minor structural protein		5836
4.32	Putative gp14-like protein	*gp14*	5832
4.31	N-acetylmuramoyl-L-alanine amidase family protein		5839
3.65	Phage tail family protein		5835
3.40	Putative major capsid protein	*gpP*	5831
2.89	Uncharacterized protein		5823
2.36	WxL domain surface cell wall-binding family protein		3215
2.34	WxL domain surface cell wall-binding family protein		3217
2.33	Phage antirepressor KilAC domain protein		5855
2.30	Dihydropteroate synthase	*folP*	2448
2.19	Zinc-binding dehydrogenase family protein		318
2.07	WxL domain surface cell wall-binding family protein		3218
1.95	Toxic anion resistance family protein		2068
	25 °C > 37 °C at stationary phase		
7.83	Thermolysin metallopeptidase, catalytic domain protein		5317
4.86	Transglutaminase-like superfamily protein		1487
4.54	UDP-N-acetylglucosamine 1-carboxyvinyltransferase	*murA*	2685

4.51	Ribonuclease J	*rnjA*	2375
4.51	Ornithine aminotransferase	*rocD*	1349
4.16	Pyruvate carboxylase	*pyc*	4104
4.10	Malic enzyme, NAD binding domain protein		3400
4.01	CTP synthase	*pyrG*	2681
3.95	Glycerophosphoryl diester phosphodiesterase family protein		4572
3.73	Leucine--tRNA ligase	*leuS*	3254
3.66	Viral enhancin family protein		2918
3.66	Subtilase family protein		4301
3.16	50S ribosomal protein L2	*rplB*	2391
3.16	Aldo/keto reductase family protein		2308
3.14	Sphingomyelin phosphodiesterase	*sph*	1822
	37 °C > 25 °C at stationary phase		
9.19	Chitinase A1	*chiA1*	2089
7.85	Putative hydrolase		2662
7.31	Glucanase		5335
6.99	Collagenase family protein		4546
5.67	Chitinase A		4342
4.83	Peptide ABC transporter		2309
4.54	Calcineurin-like phosphoesterase family protein		4913
4.43	Urocanate hydratase	*hutU*	4415
4.31	Single-stranded DNA-binding protein	*ssb*	2546
4.28	Matrixin family protein		4915
3.77	3-hydroxyacyl-[acyl-carrier-protein] dehydratase FabZ	*fabZ*	2750
3.56	Formate acetyltransferase	*pflB*	2025
3.52	Ribose-phosphate pyrophosphokinase	*prs*	2472
3.26	Putative phage major capsid protein		5824
3.22	50S ribosomal protein L4	*rplD*	2393

Temperature-dependent cell proteome analysis of exponentially growing *Bc*G9241 cells. The greatest temperature-dependent change in secreted toxin profiles was seen in exponentially growing cells. Therefore, to investigate the potential role of PlcR in the temperature-dependent regulation of toxin secretion, and any relationship between protein synthesis and secretion, a proteomic analysis of whole cells was performed. The same samples used for the supernatant proteomic analysis were used for this, allowing for direct correlation of the datasets. The full datasets generated can be seen in the **Supplementary Dataset S3.**

No build-up of toxins was observed in the cellular proteome of *Bc*G9241 at 37 °C exponential phase. With a cut-off criteria of p-value < 0.05 and a minimum 2-fold change in protein level, 67 proteins were found to be significantly more abundant at 25 °C compared to 37 °C. The most abundant proteins at 25 °C compared to 37 °C included cold shock proteins CspA and YdoJ family proteins (**Table 2** and **Fig S5**). Only two of the toxin proteins seen at higher levels at 25 °C in comparison to 37 °C in the secretome were also significantly higher in the cell proteome, NheA and NheB (AQ16_659 and 660).

51 proteins were found to be significantly more abundant at 37 °C compared to 25 °C (**Table 2**). Proteins from an operon of WxL-domain cell wall-binding proteins were seen to be more abundant at 37 °C

244 (AQ16_3217 – 3219). In addition, various heat stress response proteins were also identified as higher
245 at 37 °C. These include: AQ16_3857, a DNA repair protein; AQ16_512, a DNA protection protein and
246 a thermosensor operon, AQ16_3712 – 3714, involved in protein refolding. Interestingly, despite the
247 significantly increased abundance in the secretome, only two proteins encoded on the pBFH_1
248 phagemid (AQ16_5849 and _5858) showed increased abundance in the cell proteome, both of which
249 are uncharacterised.
250
251 A build-up of toxins from the cell proteome at 37 °C was not observed, demonstrating that temperature-
252 dependent toxin expression is not regulated at the level of secretion. PlcR was detected at both
253 temperatures with no significant difference in abundance levels.

254 **Table 2:** Top 15 cellular proteins that are more abundant at each temperature in exponentially growing
255 *Bc*G9241. The significance cut-off criteria used was a p-value of <0.05 and a minimum 2-fold change
256 in protein level.

Log_2-Fold Change	25 °C > 37 °C at exponential phase	Gene	Gene Loci (AQ16_)
5.09	Major cold shock protein	*cspA*	1368
4.72	Uncharacterized protein		4251
4.48	Cold-inducible YdjO family protein		175
4.10	Uncharacterized protein		4821
3.18	Transglutaminase-like superfamily protein		1487
3.06	Flagellar motor switch FliM family protein		858
2.77	FMN-dependent NADH-azoreductase	*azoR4*	2611
2.57	Uncharacterized protein		1372
2.47	Hemolytic enterotoxin family protein		659
2.41	Uncharacterized protein		1559
2.21	Major cold shock protein	*cspA*	174
2.20	SET domain protein		2908
2.19	Transposase family protein		1725 / 4355
2.15	Rhodanese-like domain protein		1704
2.09	Hemolytic enterotoxin family protein	*nheA*	660
	37 °C > 25 °C at exponential phase		
4.34	WxL domain surface cell wall-binding family protein		3218
3.74	Uncharacterized protein		3219
2.87	Formate acetyltransferase	*pflB*	2025
2.73	Uncharacterized protein		1429
2.29	DNA repair protein	*recN*	3857
2.27	DNA protection during starvation protein 1	*dps1*	512
2.25	Uncharacterized protein		5765
2.25	Pyruvate formate-lyase-activating enzyme	*pflA*	2024
2.23	L-lactate dehydrogenase	*ldh*	3111
2.166	CamS sex pheromone cAM373 family protein		2171
2.09	L-asparaginase, type I family protein		4939
1.98	Heat-inducible transcription repressor	*hrcA*	3712
1.97	Uncharacterized protein		5849
1.96	Membrane MotB of proton-channel complex MotA/MotB family protein		3490
1.84	Periplasmic binding family protein		1888

257

258 **Analysis of PlcR-controlled toxin expression in *Bc*G9241.** Haemolytic and cytolytic
259 assays have suggested that *Bc*G9241 containing a functional copy of the *plcR* gene show temperature-
260 dependent toxicity. Hbl, Nhe, Plc, CytK and a thermolysin metallopeptidase (AQ16_5317), which are
261 regulated by the PlcR-PapR circuit (16), were detected with high abundance in the secretome analysis
262 at 25 °C compared to 37 °C. In order to confirm the temperature-dependent toxin and protease

263 production, a panel of transcription-translation reporter plasmids were made, in which the promoter
264 regions and the first 24 bp of the coding sequence of *hbl, nhe, plc, cytK* and *AQ16_5317* were
265 genetically fused in frame to a *gfp* gene with no start codon (referred to hereon as *hbl::gfp, nhe::gfp,*
266 *plc::gfp, cytK::gfp* and *AQ16_5317::gfp*). Note that only eight N-terminal amino acids from the ORF
267 were cloned as it is not sufficient to serve as a Sec-dependant secretion signal for the toxins, preventing
268 the GFP from being secreted. For comparison, GFP reporters of PlcR-regulated toxins were also
269 constructed for *Bc*ATCC14579 from homologous regions. Each of the reporter constructs were then
270 transformed into the relevant *B. cereus* strain and examined using fluorescence microscopy and
271 microtitre plate reader assays to assess the expression patterns across growth phases at 25 °C and 37
272 °C, when grown in LB while maintaining plasmid marker selection. The rate of change in fluorescence
273 (ΔGFP/OD_{600}) was calculated every hour by subtracting the fluorescence at a given time point by the
274 fluorescence of the previous time point. This would reveal when the biggest change in GFP expression
275 occurs across the growth phase.
276
277 From the microscopy images, the expression of the toxin reporters in *Bc*G9241 was not detected during
278 mid-exponential phase at 25 °C and 37 °C (**Fig 2A** and **Fig S6**). However, by quantifying the GFP
279 intensity of *B. cereus* strains containing the reporters, there were cells with higher fluorescence
280 compared to the control cells (being above the threshold), suggesting that GFP, and therefore the PlcR-
281 regulated proteins were being expressed. The mean GFP intensity of individual cells quantified was
282 higher at 25 °C compared to 37 °C for *hbl::gfp*, *nhe::gfp* and *cytK::gfp* (**Fig S8**). Once reaching stationary
283 phase, the difference in the expression of the toxin reporters in *Bc*G9241 was more pronounced
284 between 25 °C and 37 °C (**Fig 2A** and **Fig S6**). From GFP intensity quantification of individual cells
285 from the micrographs, the mean GFP intensity of *hbl::gfp, nhe::gfp, plc::gfp* and *AQ16_5317::gfp* at the
286 onset of stationary phase and 24 hours was higher at 25 °C compared to 37 °C in *Bc*G9241 (**Fig S7**).
287 It is interesting to note that *Bc*G9241 cells formed filamentous-like structures during exponential phase
288 which reverted to shorter vegetative rod morphologies once stationary phase was reached.
289
290 When the GFP intensity/OD_{600} of *Bc*G9241 harbouring the PlcR-regulated toxin reporters was
291 monitored with a microtitre plate reader over 24 hours (**Fig 2B** and **Fig S6**), the GFP expression was
292 greater at 25 °C compared to 37 °C for *hbl::gfp, nhe::gfp, plc::gfp* and *AQ16_5317::gfp* while the
293 expression of *cytK::gfp* appeared similar between both temperatures. By calculating the rate of change
294 in fluorescence (ΔGFP), a large and broad ΔGFP peak was observed at 25 °C while the peak appeared
295 tighter at 37 °C for *hbl::gfp, nhe::gfp, plc::gfp* and *AQ16_5317::gfp* (**Fig S8**). In comparison, expression
296 of *hbl::gfp*, *nhe::gfp* and *BC_2735::gfp* (BC_2735 has a 97% identity to AQ16_5317 using BLASTP) in
297 *Bc*ATCC14579 appeared to be similar at 25 °C and 37 °C, while the expression of *plc::gfp* and *cytK::gfp*
298 was temperature-dependent (**Fig S9**).

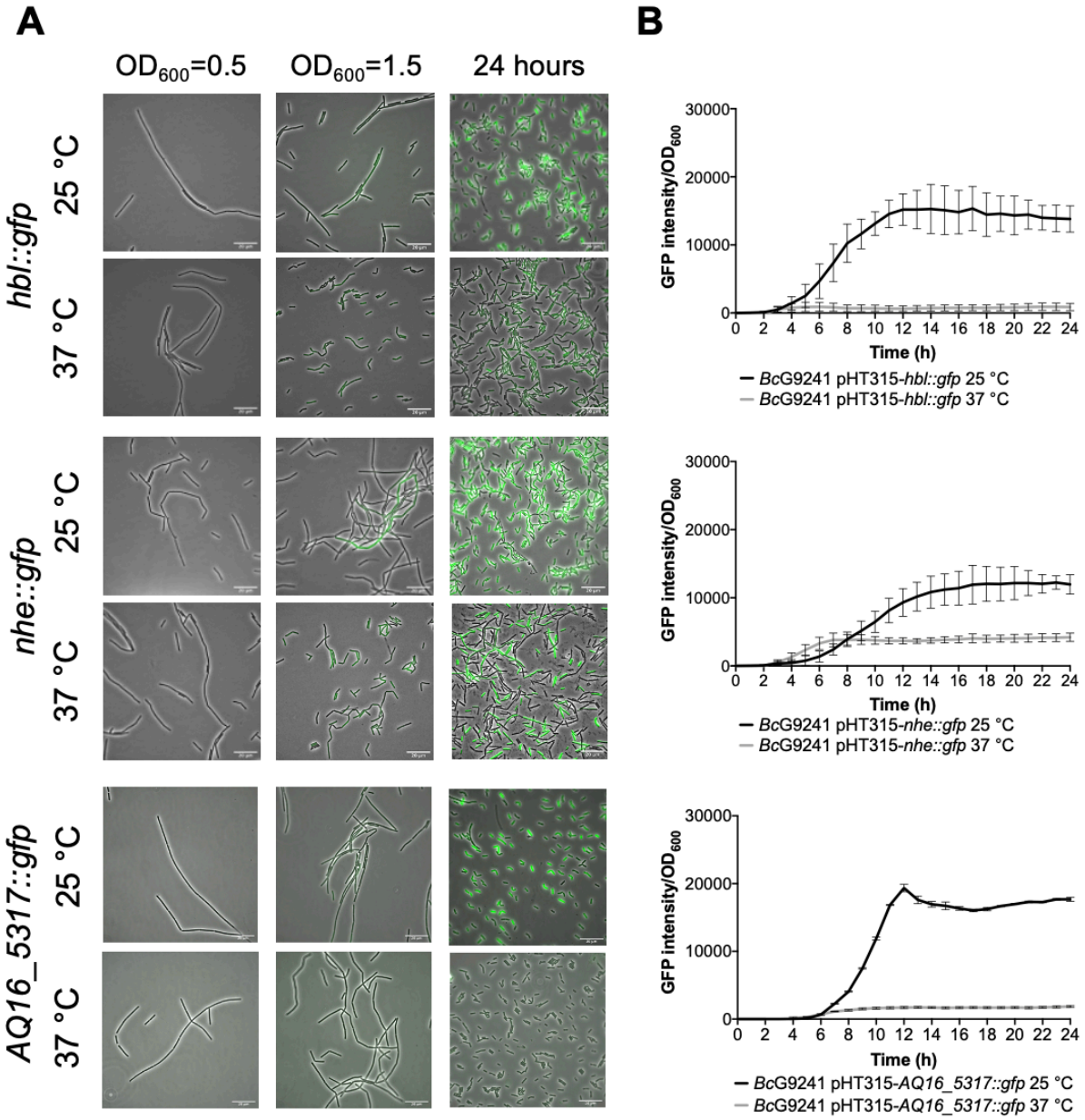

Figure 2: **Temperature dependent expression of PlcR-regulated toxins and enzymes in *Bc*G9241 using GFP reporters.** (**A**) A representative selection of microscopy images of the transcription-translation GFP reporters of PlcR-regulated toxins for *Bc*G9241 taken at three different time points: mid-exponential phase which is 2 hours at 37 °C and 5 hours at 25 °C (OD_{600}=0.5), early stationary phase which is 4 hours at 37 °C and 7 hours at 25 °C (OD_{600}=1.5) and 24 hours. (**B**) **Fluorescence of toxin reporters over time in LB.** GFP intensity/OD_{600} and change in GFP (ΔGFP/OD_{600}) of *Bc*G9241 containing PlcR-regulated toxin reporters over 24 hours growth in 100 µl volume LB media at 25 °C (in black) and 37 °C (in grey). Each line represents the mean of three biological replicates with three technical replicates each and error bars denote standard deviation.

310 **Population level analysis of PlcR and PapR expression in *Bc*G9241.** Subsequently,
311 we expanded the analysis by including a panel of transcription-translation reporter plasmids for PlcR
312 and PapR in *Bc*G9241 and *Bc*ATCC14579. The promoter regions and the first 24 bp of the coding
313 sequence of *plcR* and *papR* were genetically fused in frame to a *gfp* gene with no start codon (referred
314 to hereon as *plcR::gfp* and *papR::gfp*). Note that only eight N-terminal amino acids from the ORF were
315 cloned as it is not sufficient to serve as a Sec-dependent secretion signal for PapR and to make sure
316 that the PlcR protein was not interfering with the GFP protein. Each of the reporter constructs were then
317 transformed into the relevant *B. cereus* strain and examined using fluorescence microscopy to assess
318 the expression patterns across growth phases at 25 °C and 37 °C, when grown in LB and maintaining
319 plasmid marker selection.
320
321 **Expression of PlcR is not temperature dependent.** Expression of *plcR::gfp* was first observed during
322 early stationary phase at 25 °C and 37 °C (**Fig 3A**). By 24 hours, levels of *plcR::gfp* increased at both
323 temperatures, with a high level of population heterogeneity in expression within the cell population. The
324 cells that expressed *plcR::gfp*, also did so at a high level. As observed in *Bc*G9241, expression of
325 *plcR::gfp* in *Bc*ATCC14579 was also heterogeneous within the cell population (**Fig 3A**). Image analysis
326 provided an objective quantification of this heterogeneous expression observed within the cell
327 population, with a small number of cells expressing *plcR::gfp* in both *B. cereus* strains (**Fig S10**).
328
329 There is a possibility that the population heterogeneity observed for the expression of *plcR::gfp* could
330 be due to cell death or an error from the reporter itself. To determine whether the *plcR::gfp* expression
331 was indeed originated from a minority of cells, some potential issues were analysed. The shuttle vector
332 used for the reporter pHT315 encodes an erythromycin resistance gene, and therefore the antibiotic
333 was added to maintain selection. To rule out heterogeneity due to cell death, propidium iodide staining
334 was carried out. Cell viability is assessed when propidium iodide penetrates damaged membranes
335 binding to nucleic acid, leading to fluorescence. At early stationary phase, only a few cells were stained
336 by propidium iodide while within a large population of live cells, a small proportion of cells expressed
337 *plcR::gfp* (**Fig S11**). This confirms the heterogeneous expression of *plcR::gfp* was indeed originated
338 from a small subpopulation of live cells and this is not a consequence of cell death in any non-reporter
339 expressing cells.
340
341 **PapR in *Bc*G9241 is highly expressed at 37 °C compared to 25 °C.** Expression of *papR::gfp* was
342 first noticed during early stationary phase at 25 °C and 37 °C. Levels of *papR::gfp* expression greatly
343 increased by 24 hours, with stronger fluorescence observed by microscopy at 37 °C compared to 25
344 °C (**Fig 3B**). Image analysis has provided an assessment of the expression observed within the cell
345 population, with a sub-population of cells expressing *papR::gfp* at 25 °C. In *Bc*G9241 and
346 *Bc*ATCC14579, the mean GFP expression was higher at 37 °C compared to 25 °C (**Fig S10**).

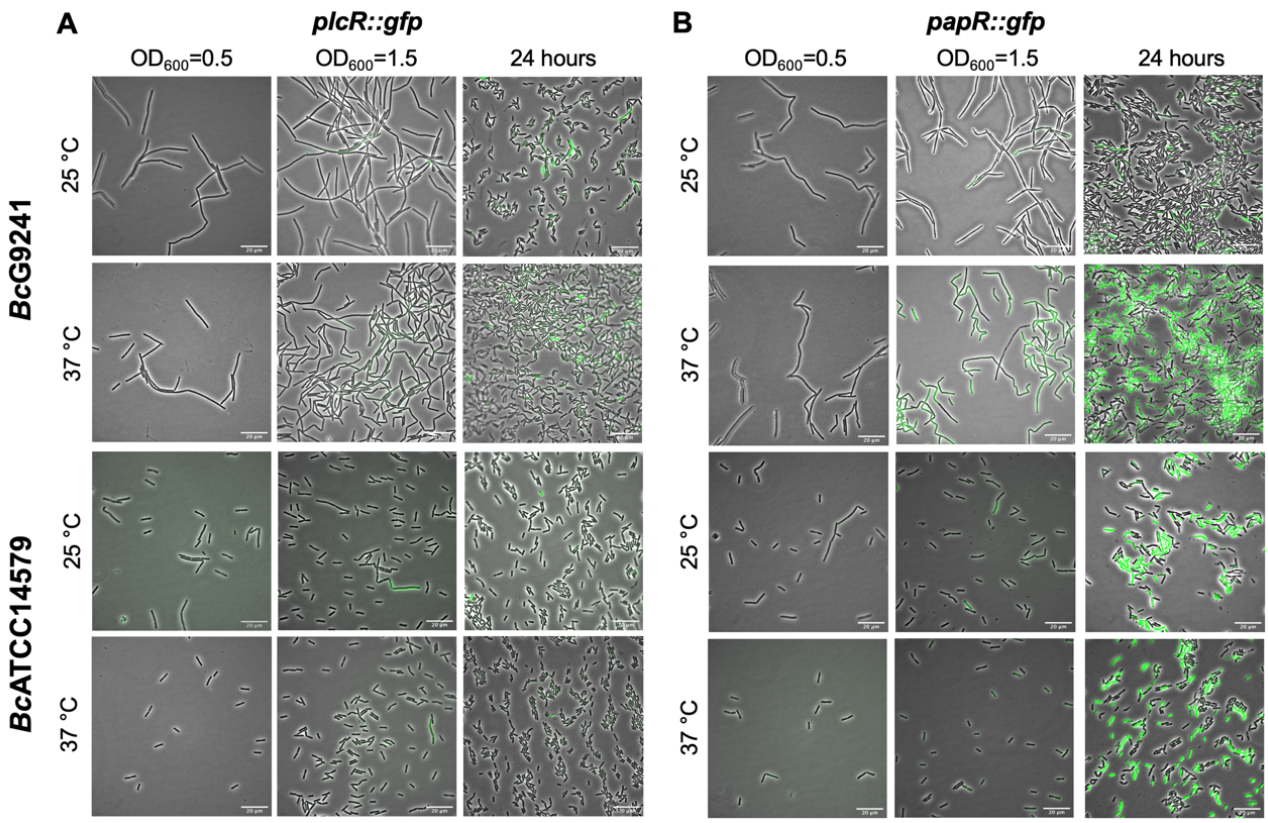

Figure 3: **A representative selection of microscopy images of BcG9241 and BcATCC14579 harbouring the transcription-translation GFP reporters of *plcR::gfp* and *papR::gfp***. Micrographs were taken at three different time points: mid-exponential phase which is 2 hours at 37 °C and 5 hours at 25 °C (OD_{600}=0.5), early stationary phase which is 4 hours at 37 °C and 7 hours at 25 °C (OD_{600}=1.5) and 24 hours. Scale bar = 20 μm.

The import of mature $PapR_7$ is functional at 25 °C and 37 °C in *Bc*G9241. A build-up of toxin proteins in the cell proteome at 37 °C was not detected, suggesting that temperature-dependent toxin expression is not regulated at the level of secretion. This led us to investigate whether the import of mature PapR is not functional at 37 °C, causing the temperature-dependent haemolysis and cytolysis phenotypes observed in *Bc*G9241. To understand whether the import system is functional at 37 °C, a haemolysis assay was carried out using supernatants of *B. cereus* cultures grown at 25 °C and 37 °C with mature synthetic PapR peptides added exogenously. Previous studies have demonstrated that the heptapeptide $PapR_7$ is the mature form of the quorum sensing peptide (22,28) and therefore synthetic peptides of this form (G9241 $PapR_7$= SDLPFEH, ATCC14579 $PapR_7$= KDLPFEY) were used.

At 25 °C, with the addition of exogenous self $PapR_7$ (i.e., adding G9241 $PapR_7$ into cultures of *Bc*G9241 or adding ATCC14579 $PapR_7$ into cultures of *Bc*ATCC14579), no significant change in haemolytic activity of the mid-exponential supernatants of *Bc*G9241 was observed, compared to the absence of exogeneous $PapR_7$. Nevertheless, haemolytic activity was still observed with/without the addition of the

363 cognate $PapR_7$ from supernatants collected at 25 °C in both *Bc*G9241 and *Bc*ATCC14579 (**Fig 4**). In
364 comparison, upon the addition of exogenous PapR a significant change in haemolytic activity of the
365 mid-exponential supernatant of *Bc*ATCC14579 was observed, compared to the absence of exogeneous
366 $PapR_7$. At 37 °C, with the addition of cognate $PapR_7$, there was a significant increase in haemolytic
367 activity with the mid-exponential and stationary phase *Bc*G9241 supernatant (**Fig 4)**. This suggests that
368 $PapR_7$ can get taken into the cell through an import system at 37 °C. In comparison, upon the addition
369 of exogenous cognate $PapR_7$, no significant change in haemolytic activity of the mid-exponential
370 supernatant of *Bc*ATCC14579 was observed, compared to the absence of exogeneous $PapR_7$.
371
372 Addition of exogenous non-self $PapR_7$ molecules in *Bc*G9241 and *Bc*ATCC14579 (i.e., adding G9241
373 $PapR_7$ into cultures of *Bc*ATCC14579 or adding ATCC14579 $PapR_7$ into cultures of *Bc*G9241) led to a
374 decrease in haemolytic activity at both temperatures (**Fig 4)**. This implies that the correct $PapR_7$ is
375 required for the expression of toxins, and that a non-self cognate variant of the peptide can actually
376 interfere with the native PlcR-PapR circuit.
377
378 Subsequently, we wanted to observe how the addition of the synthetic $PapR_7$ would affect the
379 expression of PlcR-regulated toxins in *Bc*G9241 at 37 °C using the GFP reporters we have available.
380 At 25 °C, addition of the cognate $PapR_7$ to *Bc*G9241 led to a slight increase in expression of *nhe::gfp*,
381 no change in expression of *plc::gfp* and *cytK::gfp* and a decrease in expression of *hbl::gfp*. A decrease
382 in the expression of *hbl::gfp* was still observed when lower concentrations of synthetic PapR were added
383 to BcG9241 cultures (data not shown). At 37 °C, addition of cognate $PapR_7$ to *Bc*G9241 led to a
384 dramatic increase in expression of Nhe, Plc and CytK. This suggests that the processed PapR can
385 indeed get imported into cells at 37 °C. There is no significant increase in *hbl::gfp* expression with the
386 addition of $PapR_7$ at 37 °C (**Fig S12)** suggesting an additional level of regulation for these genes.

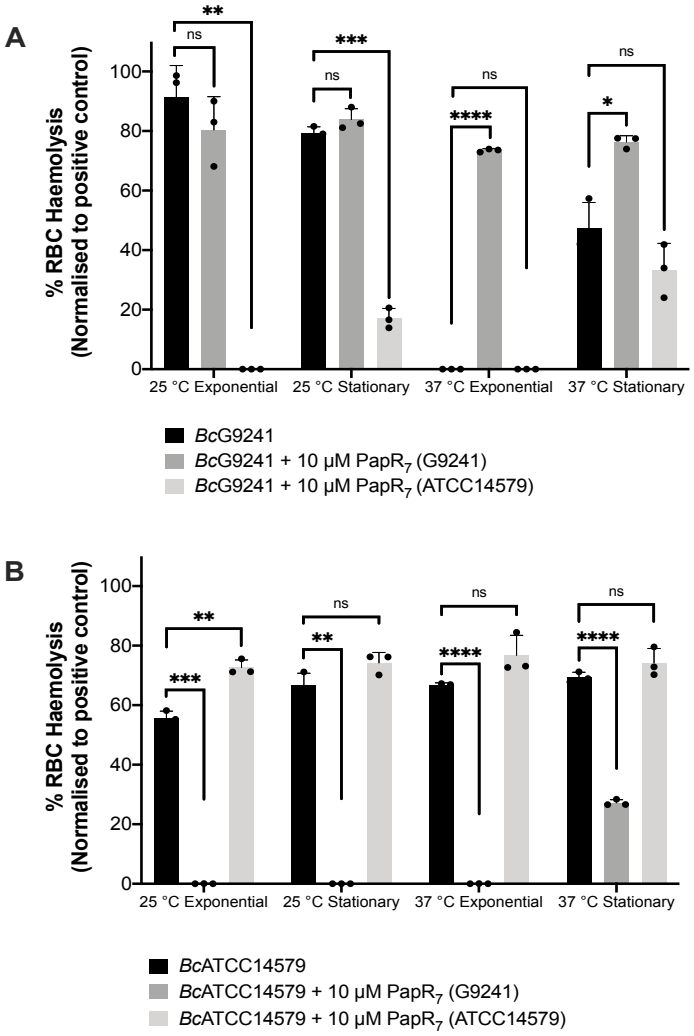

Figure 4: The effect of exogenous PapR$_7$ in *Bc*G9241 and *Bc*ATCC14579. 10 μM synthetic PapR$_7$ (G9241 PapR$_7$= SDLPFEH, ATCC14579 PapR$_7$= KDLPFEY) were added when the bacterial culture was inoculated from OD_{600}=0.005. Supernatant was extracted from mid-exponential and stationary phase growing *B. cereus* G9241. Supernatant was filter-sterilised and incubated with 4% RBCs for 1 hour. OD_{540} was measured and RBC lysis was calculated as a percentage of expected RBC lysis, normalised with 70 % lysis from 1 % (w/w) Triton X-100. Error bars denote one standard deviation, and all samples were to an n=3. * [P < 0.05], **[P < 0.01], ***[P < 0.001] and ****[P < 0.0001] as determined by unpaired t-test, with Welch's correction.

The PapR maturation process is potentially preventing the expression of PlcR-controlled toxins in *Bc*G9241 at 37 °C. The import of mature PapR does not appear to be a limiting factor involved in the temperature-dependent toxin expression phenotype. Consequently, there is a possibility that the protease(s) involved in processing PapR represents the limiting step within the PlcR-PapR circuit in *Bc*G9241. In *B. cereus,* it has been shown that the neutral protease NprB is involved in processing the pro-peptide PapR$_{48}$ into the shorter and active form PapR$_7$ (22). In the *B. cereus* and *B. thuringiensis* genome, the gene *nprB* is found adjacent to *plcR* and transcribed in the opposite orientation (6,21,22). To identify whether *Bc*G9241 and other *B. cereus-B. anthracis* "cross-over" strains have a functional copy of *nprB,* a synteny analysis using SyntTax

405 (https://archaea.i2bc.paris-saclay.fr/SyntTax/Default.aspx) was carried out. SyntTax uses the genomic
406 and taxonomic database obtained from NCBI. The NprB protein sequence from *Bc*ATCC14579 (RefSeq
407 accession GCF_000007835.1) was used as the query protein. As shown in **Fig 5**, *Bc*G9241 as well as
408 the "cross-over" strains *B. cereus* 03BB87, *B. cereus* 03BB102, *B. cereus* BC-AK and *B. cereus* bv
409 *anthracis* CI can be seen to encode only remnants of the *nprB* gene located near the *plcR-papR* operon,
410 with low synteny scores. In comparison, typical *B. cereus* sensu stricto and *B. thuringiensis* strains have
411 intact copies of *nprB*, as previously described (6,21,22) with synteny scores above 97% (**Fig 5**). *B.*
412 *anthracis* strains (Ames and Sterne) also lack the full copy of the *nprB* gene (22). This indicates that
413 NprB may not be involved in processing PapR in *B. cereus* strains carrying functional copies of both
414 *plcR* and *atxA*.
415
416 This led us to question which protease(s) is/are capable of processing PapR in *Bc*G9241 and whether
417 the temperature-dependent toxin expression in *Bc*G9241 is due to differential expression of these
418 theoretical alternative protease enzymes. From the *Bc*G9241 secretome analysis of the supernatant
419 extracted from cultures grown at 25 °C and 37 °C, several proteases were identified as highly expressed
420 at 25 °C compared to 37 °C that could potentially be involved in processing PapR in *Bc*G9241 to its
421 active form (**Table 1**). To determine whether temperature-dependent proteolytic activity is present in
422 *Bc*G9241 as suggested by the secretome analysis, a protease activity assay was carried out using skim
423 milk agar plates. Filtered supernatant of *Bc*G9241 grown at mid-exponential phase 25 °C showed
424 hydrolysis of the skimmed milk casein whereas no clear zone was observed from cultures grown at
425 mid-exponential phase 37 °C, which demonstrates that there is indeed a temperature-dependent
426 protease activity deployed during mid-exponential phase of growth (**Fig 6**). Supernatants of *B. cereus*
427 cultures into which synthetic $PapR_7$ was added were also collected and spotted onto skim milk agar to
428 look for any changes in proteolytic activity. Interestingly, the addition of the synthetic $PapR_7$ peptide to
429 cultures of either *Bc*G9241 or *Bc*G9241 ΔpBCX01 led to a significant increase in proteolytic activity at
430 both temperatures (**Fig S13**), presumably caused by PlcR-regulated proteases such as the thermolysin
431 metallopeptidase (AQ16_5317), which we have shown to be highly expressed at 25 °C compared to 37
432 °C (see above).
433
434 From the secretome analysis, AQ16_5317 labelled as a thermolysin metallopeptidase was found to be
435 highly abundant at 25 °C compared to 37 °C during exponential and stationary phase (**Table 1**). Out of
436 all these proteases/enzymes listed in **Table 1**, only the gene encoding the thermolysin metallopeptidase
437 and collagenase has a PlcR-box on the promoter region. There is a possibility that AQ16_5317 is the
438 protease involved in processing PapR in *Bc*G9241. From a synteny analysis to look into whether
439 AQ16_5317 thermolysin metallopeptidase was present in other *B. cereus* species, a high synteny score
440 as shown in some of the *B. cereus-B. anthracis* "cross-over" strains, as well as *B. cereus* sensu stricto,
441 *Bacillus weihenstephanensis, B. anthracis* and *B. thuringiensis* (**Fig S14**).
442
443 To identify whether expressing AQ16_5317 at 37 °C would abolish the temperature-dependent
444 haemolytic phenotype, the AQ16_5317 ORF with a promoter not linked to the PlcR-PapR regulator

(*fusA* promoter) was cloned into the shuttle vector pHT315 which should be able to constitutively express the protease. When measuring the OD_{600} over 24 hours using a plate reader, strains containing the pHT315-*fusA*$_p$-*AQ16_5317* construct did not alter the growth of the bacteria (data not shown). A haemolysis assay using sheep erythrocytes was carried out with *Bc*G9241 strains containing the constitutively expressed AQ16_5317. Cell free culture supernatants from cultures grown at 25 °C and 37 °C from mid-exponential and stationary phase were tested in this assay. Supernatants from 25 °C mid-exponential and early stationary phase cultures showed no change in haemolytic activity, with or without the constitutive expression of *AQ16_5317.* However, at 37 °C mid-exponential phase, constitutive expression of AQ16_5317 expressed at 37 °C led to a significant increase in haemolytic activity compared to the control (**Fig 6**). The implication being that this protease is indeed capable of processing PapR at 37 °C, leading to the increased expression of the PlcR regulon.

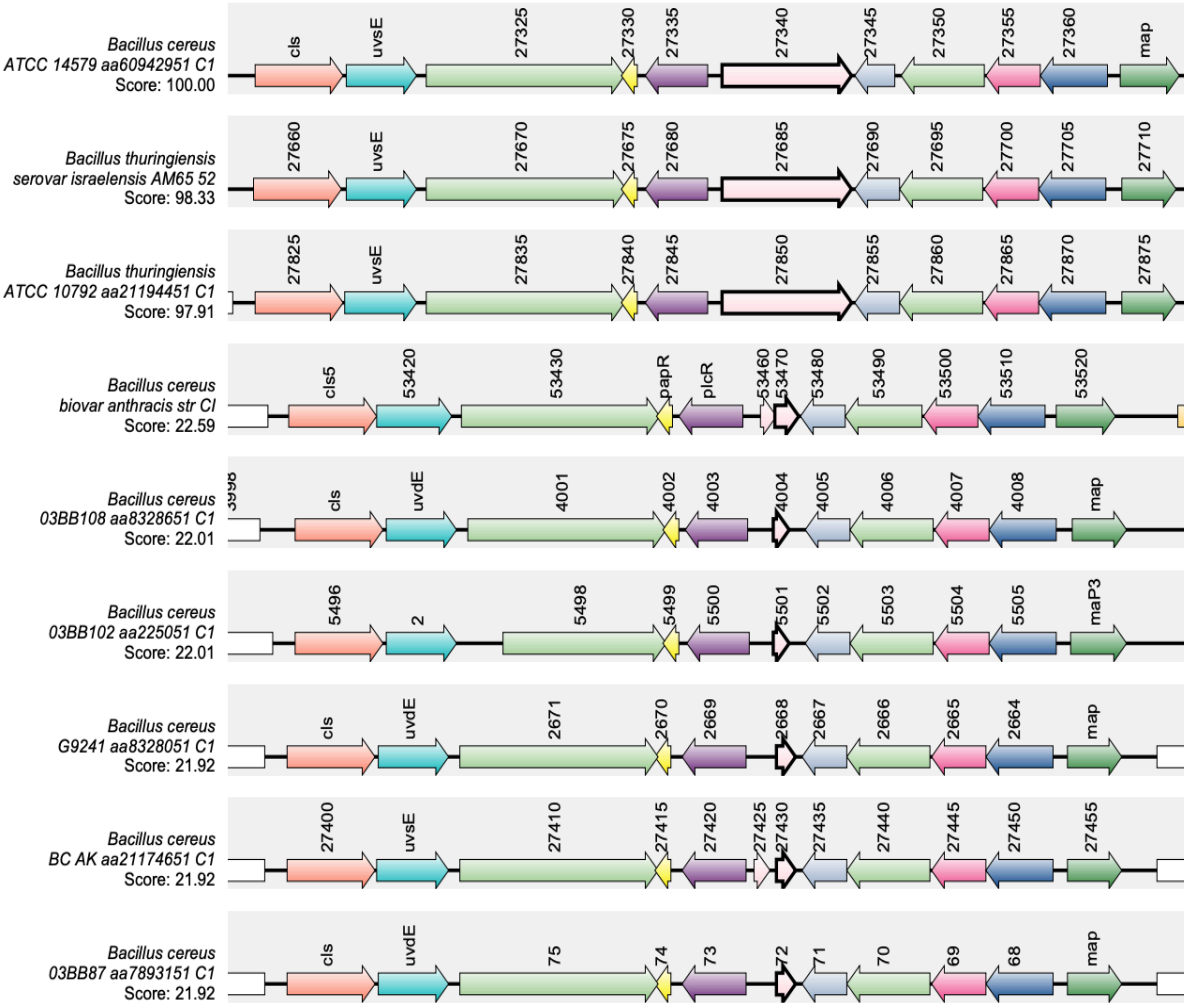

Figure 5: Synteny of the gene encoding *nprB* in *B. cereus* sensu stricto, *B. thuringiensis, B. weihenstephanensis, B. cereus* "cross-over" strains and *B. anthracis.* The NprB protein sequence from *Bc*ATCC14579 (RefSeq accession GCF_000007835.1) was used as the query protein. The gene encoding *nprB* is shown in pink with a bold border, *plcR* and *papR* are shown in purple and yellow, respectively. SynTax, a synteny web service, was used to look in the conservation of gene order (https://archaea.i2bc.paris-saclay.fr/SyntTax/Default.aspx).

463

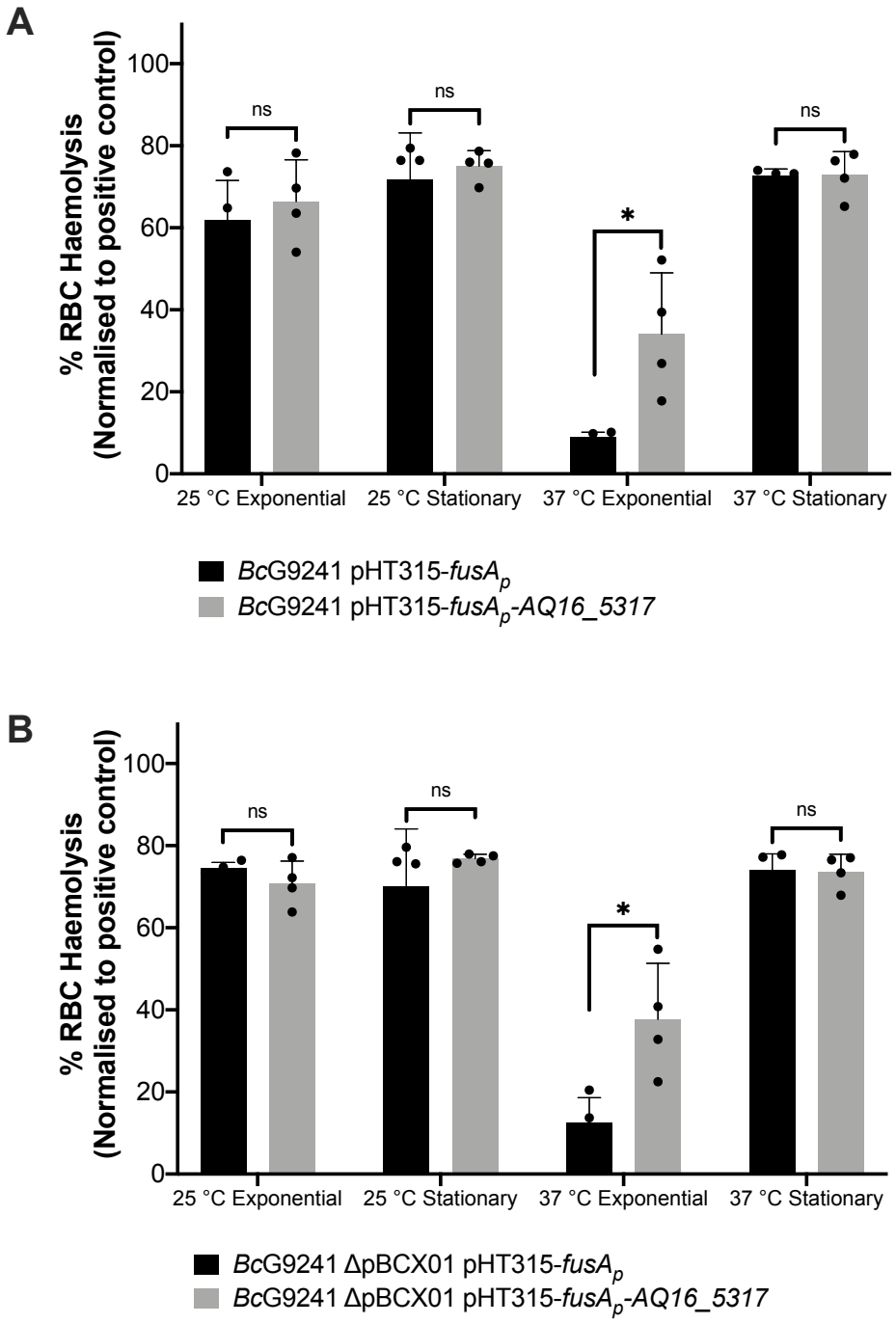

464

465 **Figure 6: Slight increase in haemolytic activity with the presence of AQ16_5317 at 37 °C during**
466 **exponential phase.** The haemolysis assay was conducted by incubating the supernatant of (**A**)
467 *Bc*G9241 and (**B**) *Bc*G9241 ΔpBCX01 with 4% RBC for one hour at 37 °C. OD_{540} was measured and
468 RBC lysis was calculated as a percentage of expected RBC lysis, normalised with 70 % lysis from 1 %
469 (w/w) Triton X-100. Stars above columns represent significance levels: * [$P < 0.05$] as determined by
470 unpaired t-test, with Welch's correction. Error bars denote one standard deviation, and all samples were
471 to an n=4.

472

473 # DISCUSSION

474 The roles and expression of PlcR and AtxA are relatively well defined in *B. cereus* and *B. anthracis,*
475 respectively. In *B. anthracis,* AtxA transcription and accumulation are enhanced at 37 °C compared to
476 28 °C (49). In *B. cereus* and *B. thuringiensis*, PlcR transcription has been observed at the onset of
477 stationary phase, suggesting cell density is required for transcription of the regulon (6,50). Also, the *B.*
478 *weihenstephanensis* KBAB4 is reported to exhibit temperature-dependent production of PlcR and PlcR-
479 regulated toxins (51). However, due to the rare nature of some *B. cereus* strains containing both *plcR*
480 and *atxA* (9,10,38–42), the understanding of how a bacterium such as *Bc*G9241 has incorporated two
481 hypothetically conflicting virulence regulators (8) has not yet been studied in detail.

482 Haemolysis and cytolysis assays using the supernatant of *Bc*G9241 demonstrated lytic activity at 25
483 °C but not at 37 °C. The supernatant of *Bc*G9241 ΔpBCX01 also demonstrated temperature-dependent
484 haemolytic and cytolytic activity, suggesting that this phenotype is not dependent on the pBCX01
485 virulence plasmid encoding AtxA1. In comparison, the supernatant of *Bt* Cry$^-$ *ΔplcR* and *Ba St* showed
486 little or no cytotoxicity against a variety of eukaryotic cells at both temperatures. As *Bt* Cry$^-$ *ΔplcR* and
487 *Ba St* lack a functional *plcR* gene, it supports the hypothesis that PlcR-regulated toxins are responsible.
488 Together these findings led us to propose that *Bc*G9241 'switches' its phenotype from a haemolytic *B.*
489 *cereus*-like phenotype at 25 °C to a non-haemolytic *B. anthracis*-like phenotype at 37 °C.

490

491 The differential cytotoxicity pattern appears to be caused by the secretion of multiple cytolytic and
492 haemolytic toxins at 25 °C, which includes Hbl, Nhe, Plc, CytK and a thermolysin metallopeptidase
493 encoded by AQ16_5317, detected from the secretome analysis of exponentially grown *Bc*G9241 cells.
494 All the corresponding genes encode an upstream PlcR box sequence (**Table S1**) and are known to be
495 transcriptionally regulated by PlcR in *Bc*ATCC14579 (7,27). Using transcription-translation GFP
496 reporters, we were able to confirm that *hbl::gfp, nhe::gfp, plc::gfp* and *AQ16_5317::gfp* are expressed
497 in a temperature dependent manner, with higher expression at 25 °C in *Bc*G9241. This was also
498 observed in *Bc*G9241 ΔpBCX01 (data not shown), further confirming that the temperature-dependent
499 toxin production is independent of the virulence plasmid. In contrast, the expression of *hbl::gfp, nhe::gfp*
500 and *BC_2735::gfp* in *Bc*ATCC14579 were at a similar level between the two temperatures. Expression
501 of *cytK::gfp* in *Bc*G9241 was heterogeneous within the cell population, which Ceuppens *et al* (2012)
502 also observed in *Bc*ATCC14579 using a cyan fluorescent protein reporter (52).
503

504 Interestingly, the most abundant proteins from the secretome analysis at 37 °C were phage proteins
505 from the pBFH_1 phagemid. This is in agreement with the transcriptomic data carried out by our group
506 (13), where high transcript levels of genes encoded on the pBFH_1 phagemid were identified at 37 °C
507 compared to 25 °C from mid-exponentially grown *Bc*G9241 cells. It is possible that the expression of
508 phage proteins might be interfering with normal PlcR-regulon toxin production. However, at this stage

509 we have not confirmed whether phage protein expression is the cause or the effect of a loss of PlcR-
510 mediated toxin expression at 37 °C, or indeed entirely independent.
511
512 The cell proteome analysis of mid-exponentially grown *Bc*G9241 cells revealed no accumulation of
513 toxins at 37 °C, implying that temperature-dependent toxin expression is not regulated at the level of
514 secretion. Also, PlcR was detected at both temperatures from the cell proteome analysis with no
515 significant difference between expression levels. Consequently, it can be concluded that the
516 temperature-dependent toxin profile is not due to levels of PlcR in the cell. Instead, this suggests that
517 the control point for temperature-dependent toxin secretion could be due to differential activity of the
518 PlcR-PapR active complex.
519
520 In *Bc*G9241 and *Bc*ATCC14579, expression of PlcR using transcription-translation GFP reporters was
521 first observed at the onset of stationary phase, in agreement with previous observations in *B.*
522 *thuringiensis* (6). Expression of PlcR was highly heterogeneous during the onset of stationary phase
523 and by 24 hours. As PlcR is under the direct- and indirect influence of other transcriptional regulators
524 such as Spo0A and CodY (27,53), it is possible that these regulators play a role in the heterogeneous
525 expression of PlcR. Phosphorylated Spo0A is able to inhibit the expression of PlcR due to the presence
526 of two Spo0A-boxes between the PlcR box in the promoter region of *plcR* (27), while CodY controls the
527 Opp system involved in importing processed PapR into the cell to activate PlcR (53). Population
528 heterogeneity between genetically identical cells could be beneficial in order to survive, persist in
529 fluctuating environment or be helpful for division of labour between cells. Transcription-translation
530 expression of PapR using GFP reporters was also observed across the growth phase. Unexpectedly,
531 expression of PapR in *Bc*G9241 increased dramatically at 37 °C, with a near homogenous expression
532 observed by 24 hours. This is in contrast with what is observed in *Bc*ATCC14579, where the expression
533 of PapR was heterogeneous at 25 °C and 37 °C. It is possible that at 37 °C, *Bc*G9241 cells are trying
534 to compensate the low expression of the PlcR regulon by expressing PapR highly.
535
536 As analysis of the cell proteome did not show a build-up of toxins at 37 °C, we wanted to identify whether
537 the temperature-dependent toxin production was caused by a limiting step within the PlcR-PapR
538 regulatory circuit in *Bc*G9241: import of mature PapR or processing of immature PapR.
539
540 Addition of synthetic $PapR_7$ to *Bc*G9241, which would bypass the secretion and processing of the full-
541 length peptide restored haemolytic activity at 37 °C. Supplementing the non-cognate form of the $PapR_7$
542 peptide into *B. cereus* strains led to suppression of haemolytic activity at both temperatures, confirming
543 that the activating mechanism of PlcR-PapR is strain specific. This observation has been previously
544 noted in *B. thuringiensis* (28). Using the PlcR-regulated toxin reporter strains made in this study, the
545 addition of synthetic $PapR_7$ led to an increase in *nhe::gfp, plc::gfp* and *cytK::gfp* expression at 37 °C in
546 *Bc*G9241. This further confirms that the mature form of PapR can be imported into the cell at 37 °C in
547 order to bind to PlcR and express the PlcR regulon. There was no significant increase in *hbl::gfp*
548 expression at 37 °C with the addition of $PapR_7$. This suggests that Nhe, Plc and CytK are responsible

549 for the haemolytic activity of *Bc*G9241 observed at 37 °C in the presence of $PapR_7$ (**Fig 4**). Intriguingly,
550 the addition of $PapR_7$ at 25 °C led to a decrease in the expression of *hbl::gfp* in *Bc*G9241. There is a
551 possibility that there are other regulators that play a role in the expression of this enterotoxin such as
552 ResDE (redox regulator), FnR, RpoN and Rex (54,55). It has been demonstrated that FnR, ResD and
553 PlcR are able to form a ternary complex *in vivo* (56), which could explain the decrease of Hbl expression
554 when synthetic $PapR_7$ were added.
555
556 Finally, this led us to question as to whether the processing of PapR by an extracellular protease(s)
557 was the limiting step causing the temperature-dependent toxin expression. The gene *nprB*, which
558 encodes for the neutral protease involved in processing PapR in *B. cereus* and *B. thuringiensis* is
559 truncated in *B. anthracis* (22), as well as in *Bc*G9241 and some of the *B. cereus-B. anthracis* "cross-
560 over" strains that carry functional copies of *plcR-papR* and *atxA* (9,10,38–42). The loss of a functional
561 copy of *nprB* may have contributed to the accommodation of *atxA* in these strains and potentially
562 allowed *B. cereus-B. anthracis "*cross-over" strains to carry both regulators. Temperature-dependent
563 proteolytic activity was observed using the supernatant of *Bc*G9241, suggesting that the processing of
564 PapR by extracellular proteases may be temperature-dependent manner. From the secretome analysis
565 of *Bc*G9241, AQ16_5317, a thermolysin metallopeptidase, was found to be one of the most highly
566 expressed proteases at 25 °C compared to 37 °C. Constitutive expression of AQ16_5317 led to a slight
567 increase in haemolytic activity at 37 °C, suggesting that AQ16_5317 is capable of processing PapR into
568 its mature form leading to the expression of PlcR-regulated toxins. The reason for not observing a
569 similar level of haemolytic activity as observed using the supernatant extracted from 25 °C growth
570 culture could be that AQ16_5317 may require further processing in order to be in its active form or is
571 not stable enough to carry out its function at 37 °C. It is also likely that though AQ16_5317 is able to
572 process PapR and express PlcR-regulated toxins at 37 °C, other proteases that have not been studied
573 here can also carry out this function, and therefore further analysis is required. The possibility of other
574 proteases processing immature PapR has been stated by Slamti *et al* (2014), though data have not
575 been published to support this statement (57).
576
577 Overall, this study reveals that haemolytic and cytolytic activity in *Bc*G9241 is determined by
578 temperature. Lytic activity at 25 °C was accompanied by higher levels of PlcR-regulated proteins
579 including Hbl, Nhe, Plc, CytK and AQ16_5317, a thermolysin metallopeptidase. Production of these
580 virulence factors at 25 °C may be essential for the invasion of insect hosts. As shown in **Figure 7,**
581 another finding of our work is that the temperature-dependent toxin production is due to differential
582 expression of protease(s) involved in processing the immature PapR into its mature form to be
583 reimported and and then activate PlcR. This study suggests that temperature-dependent regulation of
584 the PlcR-PapR regulator allows *Bc*G9241 to accommodate a functional copy of *atxA*. We hypothesise
585 that this has led to the ability of *Bc*G9241 to switch between a *B. cereus*-like phenotype at 25 ˚C and a
586 *B. anthracis*-like phenotype at 37 ˚C. The lower activity of the PlcR regulon at 37 ˚C compared to 25 ˚C
587 could be to allow the expression of AtxA and its regulon, known to be expressed at 37 ˚C in *B. anthracis*
588 (49). The characterisation of this "cross-over" strain demonstrates that the evolution of *B. anthracis* as

589 a significant mammalian pathogen is not merely about acquisition of genetic information but is also a
590 story of the power of regulation in controlling potential incompatibilities between incumbent and newly
591 acquired systems which may be a feature of other emerging pathogens.

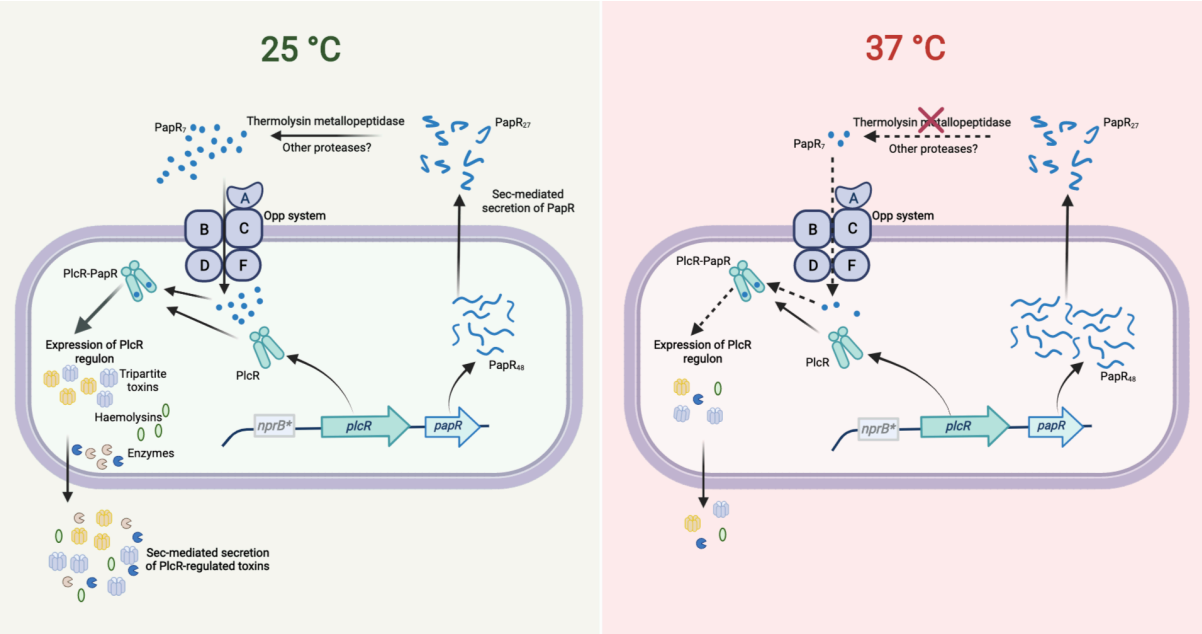

592

593 **Figure 7: The PlcR-PapR regulation circuit in *Bc*G9241 at 25 °C and 37 °C.** In *Bc*G9241, the
594 expression of *plcR* was observed at 25 °C and 37 °C, suggesting that rather than the expression of the
595 regulator, the activity of the PlcR-PapR active complex is causing differential production of PlcR-
596 regulated toxins. PapR was highly expressed at 37 °C compared to 25 °C, potentially to compensate
597 for the low expression of the PlcR regulon. Secretion of PapR was observed at both temperatures,
598 suggesting that the Sec machinery is functional at both temperatures. The import system is also
599 functional at both temperatures when $PapR_7$ is available extracellularly. Remnants of the *nprB* gene
600 (*nprB**) are present in *Bc*G9241, thus the protease NprB is not involved in the maturation of PapR as
601 observed in *B. cereus* and *B. thuringiensis*. A PlcR-regulated thermolysin metallopeptidase
602 (AQ16_5317) was identified to have the ability to process PapR and cause haemolytic activity.
603 AQ16_5317 is highly expressed at 25 °C compared to 37 °C. Diagram created with BioRender.com
604

605 # MATERIALS AND METHODS

606

607 **Bacterial strains and growth conditions.** Bacterial strains used in this study were *Bc*G9241 (9),
608 *Bc*G9241 ∆pBCX01 (13), *B. cereus* reference strain ATCC 14579 (American Type Culture Collection,
609 Manassas, Va.), the *plcR*-defective strain *B. thuringiensis* 407 Cry$^-$ ∆*plcR* (18), and *B. anthracis* Sterne
610 34F2 (pXO1$^+$, pXO2$^-$). *Bacillus* strains were cultured in 5 mL lysogeny broth (LB) at either 25 °C or 37
611 °C overnight before subculturing into 5 mL LB media. All cultures were incubated with shaking at 200
612 rpm. Larger cultures of *Bacillus* strains were cultured in 50 mL of LB unless otherwise specified. For
613 cloning, *Escherichia coli* DH5-α (NEB) and the methylation deficient *E. coli* ET12567/pUZ8002 (58)
614 were used in this study. *E. coli* strains were grown in 5 mL LB media at 37 °C, shaking at 200 rpm.
615 Media contained antibiotics when appropriate: ampicillin (100 µg/mL), chloramphenicol (25 µg/mL),
616 kanamycin (25 µg/mL) for *E. coli* and erythromycin (25 µg/mL) for *B. cereus* strains.

617

618 **Haemolysis assay.** Haemolytic activity was determined from sheep erythrocytes as described in
619 (60). Briefly, erythrocytes were diluted to 4% (vol/vol), in RPMI-1640 medium and 50 µL of this cell
620 suspension were transferred to a 96-well round-bottom polystyrene plate and incubated with 50 µL of
621 filtered supernatants of *B. cereus* cells grown to exponential (OD_{600}=0.5) or stationary phase
622 (OD_{600}=0.5). Following a 1 h-incubation at 37 ºC, lysis of human/sheep erythrocytes were determined
623 by quantifying the haemoglobin release by measurement of the absorbance at 540 nm in the resulting
624 supernatant. LB and 1% Triton X-100 were used as negative and positive control for 0% lysis and 70%
625 lysis, respectively. %RBC haemolysis was calculated as (OD_{sample} - $OD_{negative\ control}$)/($OD_{positive\ control}$ -
626 $OD_{negative\ control}$) x 70%. Assays were done by triplicate unless otherwise stated.

627

628 **Protein extraction.** Before cultures were seeded for protein extraction, pre-cultures of *Bc*G9241 were
629 used to synchronise bacterial cell growth. Pre-cultures were inoculated into 50 ml of LB broth at OD_{600}
630 = 0.005, for protein extraction. Secreted proteins were collected from mid-exponential phase or late
631 stationary phase at both 25 °C and 37 °C. Once *Bc*G9241 had grown to the appropriate time point, 6.75
632 OD units of cells were centrifuged for 5 minutes at 8000 rpm at 4 °C.

633

634 **(i) Protein extraction for secretome proteomics using in-gel digestion.** Supernatant was
635 extracted and acidified to pH 5 using 10% trifluoric acid (TFA). 50 µl of StrataClean resin (Agilent) was
636 added to each sample before vortexing for 1 minute. All samples were incubated overnight on a rotor
637 wheel mixer overnight at 4 °C for efficient protein extraction. StrataClean resin was collected by
638 centrifugation at 870 g for 1 minute. Cell supernatant was removed, and the beads resuspended in 100
639 µl of Laemlli buffer. The suspension was boiled at 95 °C for 5 minutes, to unbind the protein from the
640 resin. Beads were pelleted at 870 g for 1 minute and protein-Laemlli buffer suspension collected.

641

642 25 µl of the secreted proteins were ran on a Mini-PROTEAN® TGX™ precast gel (Bio-Rad). The whole
643 lane of the gel for each sample was sliced into 4 mm sections and washed with 1 ml of 50% ethanol in

644 50 mM ammonium bicarbonate (ABC). This wash was incubated for 20 minutes at 55 °C, shaking at
645 650 rpm. The wash solution was removed and this step was repeated twice more. The gel was
646 dehydrated in 400 µl of 100% ethanol by incubation at 55 °C for 5 minutes, with 650 rpm shaking. Once
647 the gel was dehydrated, remaining ethanol was removed. Disulphide bonds were reduced by addition
648 of 300 µl of 10 mM dithiothreitol (DTT) in 50 mM ABC. This was incubated for 45 minutes at 56 °C with
649 650 rpm shaking. DTT was removed and samples were cooled to room temperature. Cysteine residues
650 were alkylated by adding 300 µl of 55 mM iodoacetamide (IAA) in 50 mM ABC with incubation at room
651 temperature, in the dark for 30 minutes. IAA was removed and gel was washed as before by adding 1
652 ml of 50% ethanol in 50 mM and incubated at 55 °C for 20 minutes with shaking at 650 rpm. The ethanol
653 was removed and this wash was repeated twice. Gel pieces were again dehydrated with 400 µl of 100%
654 ethanol and incubated for 5 minutes at 55 °C. 200 µl of trypsin at 2.5 $ngµl^{-1}$ was added to the dehydrated
655 gel and ABC added to ensure the rehydrated gel was fully submerged. The trypsin digest was incubated
656 for 16 hours at 37 °C with 650 rpm shaking. The digest was stopped by addition of 200 µl 5% formic
657 acid in 25% acetonitrile. The solution was sonicated for 10 minutes at 35 KHz and the supernatant
658 extracted. This step was repeated three more times. A C18 stage-tip (Thermo Scientific™) was made
659 and conditioned by centrifuging 50 µl 100% methanol through the tip for 2 minutes at 2000 rpm. 100%
660 acetonitrile was washed through the tip in the same manner to equilibrate it. The tip was further
661 equilibrated with 2% acetonitrile with 1% TFA washed through the tip as before but for 4 minutes.
662 Samples were then diluted to a concentration of 10 µg of protein in 150 µl final volume of 2%
663 acetonitrile/0.1% TFA. Samples were collected on the stage tip by centrifugation through the stage tip
664 for 10 minutes under previous spin conditions. The membrane was washed with 50 µl 2%
665 acetonitrile/0.1% TFA by centrifugation at 2000 rpm for 4 minutes. Peptides were eluted in 20 µl 80%
666 acetonitrile. Samples were dried to a total volume of 40 µl at 40 °C in a speed-vac. Samples were
667 resuspended in 55 µl of 2.5% acetonitrile containing 0.05% TFA and sonicated for 30 minutes at 35
668 KHz. Samples were dried to a total volume of 40 µl at 40 °C in a speed-vac again ready for mass
669 spectroscopy. Nano liquid chromatography-electrospray ionisation-mass spectrometry (nanoLC-ESI-
670 MS)/mass spectrometry (MS) was used to carry out the analysis.
671
672 **(ii) Protein extraction for intracellular proteomics using in-urea protein digests.** Cell
673 supernatant was removed and cell pellets were suspended in 100 µl of 8M urea. Suspensions were
674 transferred to Lysing Matrix B tubes (MP Biomedicals) and cells were lysed using the FastPrep®-24
675 Classic instrument with a COOLPREP™ adapter (MP Biomedicals). Bead beating was conducted at 6
676 ms^{-1} for 40 s for 2 cycles, with a 300 s pause between cycles. Samples were filtered through
677 nitrocellulose membranes to remove the beads and protein was quantified using a Qubit 2.0 fluorometer
678 and a Qubit™ protein assay kit (Life Technologies). 50 µg of protein sample was suspended in 50 µl of
679 8 M urea buffer. 5.5 µl of 10 mM DTT was added the samples were incubated for 1 hour at room
680 temperature. 6.2 µl of 55 mM IAA was added to samples before 45 minutes incubation at room
681 temperature in the dark. Samples were then diluted to 100 µL total volume by addition of 50 mM ABC.
682 1 µg of trypsin was added to each sample per 50 µg protein and incubated for 16 hours at room
683 temperature. Samples were filtered through a C-18 stage tip as described previously and concentrated

684 to 40 µl in a speed-vac, ready for mass spectroscopy. nanoLC-ESI-MS/MS was used to carry out the
685 analysis.
686
687 **Perseus analysis of proteomics data.** The Perseus software platform (Max Planck Institute) was
688 used to analyse the highly multivariate proteomics data. Peptides only identified by site, reversed
689 peptide sequences and potential contaminants were filtered out. Secretome data was normalised by
690 the mean label-free quantification (LFQ) intensity value. Whole cell proteomics data was normalised by
691 median as the data was normally distributed. Protein hits were filtered out if they didn't have 3 values
692 in at least one condition measured. Volcano plots were plotted using a p value = 0.05 and a log2-fold
693 change = 1.
694
695 **Generation of plasmid-based transcription-translation GFP reporters**. Constructs made for this
696 study are listed on **Table S2**. Transcription-translation fusions with the *gfp* gene were constructed by
697 PCR in a pHT315 vector (59) containing *gfp* (pHT315-*gfp*). The vector was linearized using appropriate
698 restriction enzymes (NEB) and purified after agarose gel electrophoresis using the GFX^{TM} PCR DNA
699 and Gel Band Purification Kit (GE Healthcare). Insert fragments were amplified with Q5 DNA
700 polymerase (NEB) by PCR with the appropriate primer pairs listed on **Table S3**. The resulting fragments
701 were digested with the appropriate restriction enzymes, purified after agarose gel electrophoresis using
702 the GFX^{TM} PCR DNA and Gel Band Purification Kit (GE Healthcare) and ligated into
703 the linearized pHT315-*gfp* vector. Plasmid constructs were transformed into chemically competent *E.*
704 *coli* DH5-α cells through heat shock. Once confirmed by DNA sequencing, all vectors were transformed
705 into the non-methylating *E. coli* ET12567 strain by electroporation (**Supplementary Materials and**
706 **Methods**). Vectors amplified by *E. coli* ET12567 were purified and transformed into *B. cereus* strains
707 using electroporation (**Supplementary Materials and Methods**).
708
709 **Fluorescent reporter strain assays.** For growth curves and fluorescence measurements, *B. cereus*
710 strains were sub-cultured at a starting OD_{600} of 0.05 into a clear flat bottom 96-well plate (Greiner)
711 containing 100 µL of LB media per well. Cultures were grown in a FLUOstar Omega microplate reader
712 (BMG LabTech) at either 25 °C or 37 °C with continuous orbital shaking at 700 rpm. Absorbance
713 measurements (OD_{600}) and fluorescence intensity (excitation filter = 482 nm and emission filter = 520
714 nm for GFP) were taken hourly for 24 hours. Each plate contained *Bc*G9241 and *Bc*ATCC14579 strains
715 carrying GFP reporters as well as each strain carrying a control plasmid with no promoter upstream of
716 *gfp* (pHT315-*gfp*). The fluorescence of all readings was first normalized to the fluorescence of blank
717 media samples and then normalized by subtracting the autofluorescence of the corresponding control
718 strain. The rate of change in fluorescence ($\Delta GFP/OD_{600}$) using the data obtained from the microplate
719 reader was calculated by subtracting the fluorescence at a given time point by the fluorescence of the
720 previous time point:
721 $$\Delta GFP/OD_{600} = (\text{GFP intensity}_{(t)} - \text{GFP intensity}_{(t-1)})/OD_{600}$$
722

723 **Peptide Synthesis.** Peptides SDLPFEH (G9241 $PapR_7$) and KDLPFEY (ATCC14579 $PapR_7$) were
724 synthesised by GenScript (USA) at a purity >98% and diluted with sterile nuclease-free water. All
725 experiments with the use of $PapR_7$ were added at a concentration of 10 μM and during lag growth phase
726 (OD_{600} = 0.1), unless otherwise stated.
727
728 **Light and Fluorescence Microscopy.** 1 % agarose in water were made and heated using a
729 microwave until the agarose has completely dissolved. 200 μl of molten agarose was added onto a
730 microscope glass slide and a coverslip placed on top. When the agarose pad has dried and the sample
731 is ready for observation, 2 µl of sample was applied to a prepared agarose pad and a cover slip placed
732 over them. Images were captured on a Leica DMi8 premium-class modular research microscope with
733 a Leica EL6000 external light source (Leica Microsystems), using an ORCA-Flash4.0 V2 Digital CMOS
734 Camera (Hamamatsu) at 100x magnification.
735
736 **$PapR_7$ activity assay using PlcR-regulated toxin reporters.** *Bc*G9241 and *Bc*ATCC14579
737 containing PlcR-regulated toxin GFP reporters were grown overnight in LB medium with selective
738 antibiotics. Mid-exponentially grown pre-cultures of *B. cereus* strains containing PlcR-regulated toxin
739 reporters were diluted to OD_{600} 0.01 and 10 µM of $PapR_7$ were added. In a black tissue culture treated
740 96-well microtiter plate (Greiner, Scientific Laboratory Supplies), 100 µL of the culture were added in
741 each well and the GFP intensity and OD_{600} were measured every hour for over 24 hours using the
742 Omega FluoSTAR (BMG LabTech) microplate reader.
743

744 # AUTHORS AND CONTRIBUTORS

745 **Shathviga Manoharan[1]:** Planned and performed experiments and wrote much of the manuscript
746 **Grace Taylor-Joyce[1]:** Assisted in experiments and wrote parts of the manuscript
747 **Thomas Brooker[1]:** Planned and performed some of the experiments.
748 **Carmen Sara Hernandez-Rodrıguez[2]:** Planned and performed some of the experiments.
749 **Les Baillie[3]:** Provided certain bacterial strains and provided advice on handling them.
750 **Petra Oyston and Victoria Baldwin[4]:** Provided advice on handling the pathogenic strains and
751 assisted in interpreting the results.
752 **Alexia Hapeshi[1]:** Assisted in some experimental work and in interpreting certain results.
753 **Nicholas R. Waterfield[1]:** Experimental planning, secured funding, assisted in interpreting results and
754 provided guidance and edits for writing the manuscript.
755

756 [1]Division of Biomedical Sciences, Warwick Medical School, University of Warwick, Gibbet Hill Road,
757 Coventry, CV4 7AL, United Kingdom
758 [2]Institut Universitari de Biotecnologia i Biomedicina, Departament de Genètica, Facultad de Ciències
759 Biològiques, University of Valencia, 46100 Burjassot, Valencia, Spain
760 [3]School of Pharmacy and Pharmaceutical Sciences, Cardiff University, CF10 3AT, Cardiff, United
761 Kingdom

[4]CBR Division, Dstl Porton Down, Salisbury, SP4 0JQ, United Kingdom

CONFLICTS OF INTEREST

The authors declare no conflicts of interest.

FUNDING INFORMATION

This research was funded in whole or in part by the funders and grant numbers below. For the purpose of open access, the author has applied a Creative Commons Attribution (CC BY) licence (where permitted by UKRI, 'Open Government Licence' or 'Creative Commons Attribution No-derivatives (CC BY-ND) licence' may be stated instead) to any Author Accepted Manuscript version arising from this submission.

SM and **TB** were funded by the WCPRS scholarship programme provided by Warwick University, with funding contributions from Dstl (MoD) at Porton Down, UK (DSTL project references; DSTLX1000093952 and DSTLX-1000128995). **GTJ** was funded by the BBSRC MIBTP Doctoral Training Programme at the University of Warwick, UK. **CSHR** was funded by an EU Marie Curie fellowship awarded while at the University of Bath, UK (FP7-PEOPLE-2010-IEF Project 273155). **AH** was funded by a start-up financial package awarded to **NRW** upon starting at Warwick Medical School, UK. **LB** is funded by Cardiff School of Biological Sciences, UK. **PO** is funded by Dstl at Porton Down, UK. **NRW** is funded by the University of Warwick, UK.

ACKNOWLEDGEMENTS

We would like to thank the Dstl for providing funding and guidance throughout the project including valuable quarterly update meetings. We would also like to acknowledge the contribution of the WPH Proteomics Research Technology Platform (Gibbet Hill Road, University of Warwick, UK).

REFERENCES

1. Vilain S, Luo Y, Hildreth MB, Brözel VS. Analysis of the life cycle of the soil Saprophyte *Bacillus cereus* in liquid soil extract and in soil. Appl Environ Microbiol. 2006;72(7):4970–7.
2. Okinaka R, Keim P. The Phylogeny of *Bacillus cereus* sensu lato. Microbiol Spectr. 2016;4(1).
3. Carter KC. Koch's Postulates in Relation To the Work of Jacob Henle and Edwin Klebs. Med Hist. 1985;29:353–74.
4. Swiecicka I, Mahillon J. Diversity of commensal *Bacillus cereus* sensu lato isolated from the common sow bug (*Porcellio scaber*, *Isopoda*). FEMS Microbiol Ecol. 2006;56(1):132–40.
5. Granum PE, Lund T. *Bacillus cereus* and its food poisoning toxins. FEMS Microbiol Lett. 1997;157(2):223–8.
6. Lereclus D, Agaisse H, Gominet M, Salamitou S, Sanchis V. Identification of a *Bacillus thuringiensis* Gene

801 That Positively Regulates Transcription of the Phosphatidylinositol-Specific Phospholipase C Gene at the
802 Onset of the Stationary Phase. J Bacteriol. 1996;178(10):2749–56.
803 7. Agaisse H, Gomlnet M, Økstad OA, Kolstø AB, Lereclus D. PlcR is a pleiotropic regulator of extracellular
804 virulence factor gene expression in *Bacillus thuringiensis*. Mol Microbiol. 1999;32(5):1043–53.
805 8. Mignot T, Mock M, Robichon D, Landier A, Lereclus D, Fouet A. The incompatibility between the PlcR- and
806 AtxA-controlled regulons may have selected a nonsense mutation in *Bacillus anthracis*. Mol Microbiol.
807 2001;42(5):1189–98.
808 9. Hoffmaster AR, Ravel J, Rasko DA, Chapman GD, Chute MD, Marston CK, et al. Identification of anthrax
809 toxin genes in a *Bacillus cereus* associated with an illness resembling inhalation anthrax. Proc Natl Acad
810 Sci U S A. 2004 Jun 1;101(22):8449–54.
811 10. Hoffmaster AR, Hill KK, Gee JE, Marston CK, De BK, Popovic T, *et al*. Characterization of *Bacillus cereus*
812 isolates associated with fatal pneumonias: Strains are closely related to *Bacillus anthracis* and Harbor *B.*
813 *anthracis* virulence genes. J Clin Microbiol. 2006;44(9):3352–60.
814 11. Visschedyk D, Rochon A, Tempel W, Dimov S, Park HW, Merrill AR. Certhrax toxin, an anthrax-related
815 ADP-ribosyltransferase from *Bacillus cereus*. J Biol Chem. 2012;287(49):41089–102.
816 12. Fieldhouse RJ, Turgeon Z, White D, Rod Merrill A. Cholera- and anthrax-like toxins are among several
817 new ADP-Ribosyltransferases. PLoS Comput Biol. 2010;6(12).
818 13. Taylor-Joyce G, Manoharan S, Brooker T, Hernandez-Rodrıguez CS, Baillie L, Oyston P, Waterfield, N. R.
819 The influence of extrachromosomal elements in the anthrax “cross-over” strain *Bacillus cereus* G9241.
820 [Unpublished manuscript]. University of Warwick. 2022.
821 14. Hendrix RW, Casjens SR, Lavigne R. Family - Siphoviridae. Virus Taxon Ninth Rep Int Comm Taxon
822 Viruses. 2012.
823 15. Gohar M, Økstad OA, Gilois N, Sanchis V, Kolstø AB, Lereclus D. Two-dimensional electrophoresis
824 analysis of the extracellular proteome of *Bacillus cereus* reveals the importance of the PlcR regulon.
825 Proteomics. 2002;2(6):784–91.
826 16. Gohar M, Faegri K, Perchat S, Ravnum S, Økstad OA, Gominet M, et al. The PlcR virulence regulon of
827 *Bacillus cereus*. PLoS One. 2008;3(7):1–9.
828 17. Clair G, Roussi S, Armengaud J, Duport C. Expanding the Known Repertoire of Virulence Factors
829 Produced by *Bacillus cereus* through Early Secretome Profiling in Three. Mol Cell Proteomics.
830 2010;9(7):1486–98.
831 18. Salamitou S, Brehe M, Bourguet D, Gilois N, Gominet M, Hernandez E. The PlcR regulon is involved in
832 the opportunistic properties of *Bacillus thuringiensis* and *Bacillus cereus* in mice and insects. Microbiology.
833 2000;146:2825–32.
834 19. Bouillaut L, Perchat S, Arold S, Zorrilla S, Slamti L, Henry C, et al. Molecular basis for group-specific
835 activation of the virulence regulator PlcR by PapR heptapeptides. Nucleic Acids Res. 2008;36(11):3791–
836 801.
837 20. Slamti L, Gominet M, Vilas-bo G, Sanchis V, Chaufaux J, Gohar M, et al. Distinct Mutations in PlcR Explain
838 Why Some Strains of the *Bacillus cereus* Group are Nonhemolytic. J Bacteriol. 2004;186(11):3531–8.
839 21. Økstad OA, Gominet M, Purnelle B, Rose M, Lereclus D, Kolsto A-B. Sequence analysis of three *Bacillus*
840 *cereus* loci carrying PlcR-regulated genes encoding degradative enzymes and enterotoxin. Microbiology.
841 1999;145:3129–38.
842 22. Pomerantsev AP, Pomerantseva OM, Camp AS, Mukkamala R, Goldman S, Leppla SH. PapR peptide
843 maturation : Role of the NprB protease in *Bacillus cereus* 569 PlcR / PapR global gene regulation. FEMS
844 Immunol Med Microbiol. 2009;55:361–77.
845 23. Gominet M, Slamti L, Gilois N, Rose M, Lereclus D, Universita È. Oligopeptide permease is required for

846 expression of the *Bacillus thuringiensis* PlcR regulon and for virulence. Mol Microbiol. 2001;40(4):963–75.
847 24. Slamti L, Lereclus D. A cell-cell signaling peptide activates the PlcR virulence regulon in bacteria of the
848 *Bacillus cereus* group. EMBO J. 2002;21(17):4550–9.
849 25. Declerck N, Bouillaut L, Chaix D, Rugani N, Slamti L, Hoh F, et al. Structure of PlcR: Insights into virulence
850 regulation and evolution of quorum sensing in Gram-positive bacteria. PNAS. 2007;104(47):18490–5.
851 26. Grenha R, Slamti L, Nicaise M, Refes Y, Lereclus D, Nessler S. Structural basis for the activation
852 mechanism of the PlcR virulence regulator by the quorum-sensing signal peptide PapR. PNAS.
853 2013;110(3):1047–52.
854 27. Lereclus D, Agaisse H, Salamitou S, Gominet M. Regulation of toxin and virulence gene transcription in
855 *Bacillus thuringiensis*. Int J Med Microbiol. 2000;290(4–5):295–9.
856 28. Slamti L, Lereclus D. Specificity and Polymorphism of the PlcR-PapR Quorum-Sensing System in the
857 *Bacillus cereus* Group. J Bacteriol. 2005;187(3):1182–7.
858 29. Gilmore MS, Cruz-Rodz AL, Leimeister-Wachter M, Kreft J, Goebel W. A *Bacillus cereus* cytolytic
859 determinant, cereolysin AB, which comprises the phospholipase C and sphingomyelinase genes:
860 Nucleotide sequence and genetic linkage. J Bacteriol. 1989;171(2):744–53.
861 30. Lund T, Granum PE. Characterisation of a non-haemolytic enterotoxin complex from *Bacillus cereus*
862 isolated after a foodborne outbreak. FEMS Microbiol Lett. 1996;141:151–6.
863 31. Lund T, De Buyser M-L, Granum PE. A new cytotoxin from *Bacillus cereus* that may cause necrotic
864 enteritis. Mol Microbiol. 2000;38(2):254–61.
865 32. Leendertz FH, Yumlu S, Pauli G, Boesch C, Couacy-Hymann E, Vigilant L, et al. A new *Bacillus anthracis*
866 found in wild chimpanzees and a gorilla from west and central Africa. PLoS Pathog. 2006;2(1):0001–4.
867 33. Antonation KS, Grützmacher K, Dupke S, Mabon P, Zimmermann F, Lankester F, et al. *Bacillus cereus*
868 Biovar Anthracis Causing Anthrax in Sub-Saharan Africa—Chromosomal Monophyly and Broad
869 Geographic Distribution. PLoS Negl Trop Dis. 2016;10(9):1–14.
870 34. Leendertz FH, Ellerbrok H, Boesch C, Couacy-Hymann E, Mätz-Rensing K, Haken, et al. Anthrax kills wild
871 chimpanzees in a tropical rainforest. Nature. 2004;430:451–2.
872 35. Leendertz FH, Lankester F, Guislain P, Neel C, Drori O. Anthrax in Western and Central African Great
873 Apes. Am J Primatol. 2006;68:928–33.
874 36. Klee SR, Brzuszkiewicz EB, Nattermann H, Brüggemann H, Dupke S, Wollherr A, et al. The genome of a
875 *Bacillus* isolate causing anthrax in chimpanzees combines chromosomal properties of *B. cereus* with *B.*
876 *anthracis* virulence plasmids. PLoS One. 2010;5(7):e10986.
877 37. Miller JM, Hair JG, Hebert M, Hebert L, Roberts Jr. FJ, Weyant RS. Fulminating bacteremia and pneumonia
878 due to *Bacillus cereus*. J Clin Microbiol. 1997;35(2):504–7.
879 38. Sue D, Hoffmaster AR, Popovic T, Wilkins PP. Capsule production in *Bacillus cereus* strains associated
880 with severe pneumonia. J Clin Microbiol. 2006;44(9):3426–8.
881 39. Avashia SB, Riggins WS, Lindley C, Hoffmaster A, Drumgoole R, Nekomoto T, et al. Fatal Pneumonia
882 among Metalworkers Due to Inhalation Exposure to *Bacillus cereus* Containing *Bacillus anthracis* Toxin
883 Genes. Clin Infect Dis. 2007;44:414–6.
884 40. Marston CK, Ibrahim H, Lee P, Churchwell G, Gumke M, Stanek D, et al. Anthrax toxin-expressing *Bacillus*
885 *cereus* isolated from an anthrax-like eschar. PLoS One. 2016;11(6):1–7.
886 41. Wright AM, Beres SB, Consamus EN, Long SW, Flores AR, Barrios R, et al. Rapidly Progressive, Fatal,
887 Inhalation Anthrax-like Infection in a Human: Case Report, Pathogen Genome Sequencing, Pathology,
888 and Coordinated Response. Arch Pathol Lab Med. 2011;1447–59.
889 42. Pena-Gonzalez A, Marston CK, Rodriguez-R LM, Kolton CB, Garcia-Diaz J, Theppote A, et al. Draft
890 genome sequence of *Bacillus cereus* LA2007, a human-pathogenic isolate harboring anthrax-like

891 plasmids. Genome Announc. 2017;5(16).
892 43. Dupke S, Barduhn A, Franz T, Leendertz FH, Couacy-Hymann E, Grunow R, et al. Analysis of a newly
893 discovered antigen of *Bacillus cereus* biovar *anthracis* for its suitability in specific serological antibody
894 testing. J Appl Microbiol. 2019;126(1):311–23.
895 44. Dawson P, Schrodt CA, Feldmann K, Traxler RM, Gee JE, Kolton CB, et al. Fatal Anthrax Pneumonia in
896 Welders and Other Metalworkers Caused by *Bacillus cereus* Group Bacteria Containing Anthrax Toxin
897 Genes — U.S. Gulf Coast States, 1994–2020. Morb Mortal Wkly Rep. 2021;70(41):1453–4.
898 45. Baldwin VM. You Can't *B. cereus* – A Review of *Bacillus cereus* Strains That Cause Anthrax-Like Disease.
899 Front Microbiol. 2020;11(1731).
900 46. Passalacqua KD, Varadarajan A, Byrd B, Bergman NH. Comparative transcriptional profiling of *Bacillus*
901 *cereus* sensu lato strains during growth in CO_2-bicarbonate and aerobic atmospheres. PLoS One.
902 2009;4(3):1–20.
903 47. Rivera AMG, Granum PE, Priest FG. Common occurrence of enterotoxin genes and enterotoxicity in
904 *Bacillus thuringiensis.* FEMS Microbiol Lett. 2000;190(1):151–5.
905 48. Swiecicka I, Van Der Auwera GA, Mahillon J. Hemolytic and nonhemolytic enterotoxin genes are broadly
906 distributed among *Bacillus thuringiensis* isolated from wild mammals. Microb Ecol. 2006;52(3):544–51.
907 49. Dai Z, Koehler TM. Regulation of Anthrax Toxin Activator Gene (atxA) Expression in *Bacillus anthracis*:
908 Temperature , Not CO_2/ Bicarbonate, Affects AtxA Synthesis. Infect Immun. 1997;65(7):2576–82.
909 50. Brillard J, Susanna K, Michaud C, Dargaignaratz C, Gohar M, Nielsen-Leroux C, et al. The YvfTU two-
910 component system is involved in plcR expression in *Bacillus cereus*. BMC Microbiol. 2008;8:1–13.
911 51. Réjasse A, Gilois N, Barbosa I, Huillet E, Bevilacqua C, Tran S, et al. Temperature-Dependent Production
912 of Various PlcR-Controlled Virulence Factors in *Bacillus weihenstephanensis* Strain KBAB4. Appl Environ
913 Microbiol. 2012;78(8):2553–61.
914 52. Ceuppens S, Timmery S, Mahillon J, Uyttendaele M, Boon N. Small *Bacillus cereus* ATCC 14579
915 subpopulations are responsible for cytotoxin K production. J Appl Microbiol. 2012;114(3):899–906.
916 53. Slamti L, Lemy C, Henry C, Guillot A, Huillet E, Lereclus D. CodY regulates the activity of the virulence
917 quorum sensor PlcR by controlling the import of the signaling peptide PapR in *Bacillus thuringiensis*. Front
918 Microbiol. 2016;6(1501):1–14.
919 54. Duport C, Zigha A, Rosenfeld E, Schmitt P. Control of enterotoxin gene expression in *Bacillus cereus*
920 F4430/73 involves the redox-sensitive ResDE signal transduction system. J Bacteriol. 2006;188(18):6640–
921 51.
922 55. Zigha A, Rosenfeld E, Schmitt P, Duport C. The redox regulator Fnr is required for fermentative growth
923 and enterotoxin synthesis in *Bacillus cereus* F4430/73. J Bacteriol. 2007;189(7):2813–24.
924 56. Esbelin J, Jouanneau Y, Duport C. Bacillus cereus Fnr binds a [4Fe-4S] cluster and forms a ternary
925 complex with ResD and PlcR. BMC Microbiol. 2012;12(125).
926 57. Slamti L, Perchat S, Huillet E, Lereclus D. Quorum sensing in *Bacillus thuringiensis* is required for
927 completion of a full infectious cycle in the insect. Toxins (Basel). 2014;6(8):2239–55.
928 58. MacNeil DJ, Gewain KM, Ruby CL, Dezeny G, Gibbons PH, MacNeil T. Analysis of *Streptomyces*
929 *avermitilis* genes required for avermectin biosynthesis utilizing a novel integration vector. Gene.
930 1992;111(1):61–8.
931 59. Wilson MK, Vergis JM, Alem F, Palmer JR, Keane-Myers AM, Brahmbhatt TN, et al. *Bacillus cereus* G9241
932 makes anthrax toxin and capsule like highly virulent *B. anthracis* Ames but behaves like attenuated
933 toxigenic nonencapsulated *B. anthracis* Sterne in rabbits and mice. Infect Immun. 2011;79(8):3012–9.
934 60. Rudkin JK, Laabei M, Edwards AM, Joo HS, Otto M, Lennon KL, et al. Oxacillin alters the toxin expression
935 profile of community-associated methicillin-resistant *Staphylococcus aureus*. Antimicrob Agents

936 Chemother. 2014;58(2):1100–7.
937 61. Lane DL. 16S/23S rRNA sequencing. Nucleic Acid Techniques in Baclerial Syslelllalics. 1991;115–75.
938 62. Arantes O, Lereclus D. Construction of cloning vectors for *Bacillus thuringiensis*. Gene. 1991;108:115–9.
939 63. Salter RD, Cresswell P. Impaired assembly and transport of HLA-A and -B antigens in a mutant TxB cell
940 hybrid. EMBO J. 1986;5(5):943–9.
941 64. Daigneault M, Preston JA, Marriott HM, Whyte MKB, Dockrell DH. The identification of markers of
942 macrophage differentiation in PMA-stimulated THP-1 cells and monocyte-derived macrophages. PLoS
943 One. 2010;5(1).
944 65. Silva, C.P., Waterfield, N.R., Daborn, P.J., Dean, P., Chilver, T., Au, C.P.Y., Sharma, S., Potter, U.,
945 Reynolds, S.E. and Ffrench-Constant, R.H. (2002) 'Bacterial infection of a model insect: Photorhabdus
946 luminescens and Manduca sexta', *Cellular Microbiology*, 4(6), pp. 329–339.
947 66. Vlisidou I, Hapeshi A, Healey JRJ, Smart K, Yang G, Waterfield NR. The *Photorhabdus asymbiotica*
948 virulence cassettes deliver protein effectors directly into target eukaryotic cells. Elife. 2019;8:1–24.
949